Studies on virulence determinants of highly pathogenic avian influenza viruses

(高病原性鳥インフルエンザウイルスの病原性決定因子に関する研究)

Naganori Nao

CONTENTS

Abbreviations

2-ME	2-mercaptoethanol
cDNA	complementary deoxyribonucleic acid
CEF	chicken embryo fibroblasts
CHX	cycloheximide
CLC	CLC Genomic Workbench version 8.0.2
cRNA	complementary ribonucleic acid
DEF	duck embryo fibroblasts
DMEM	Dulbecco's minimal essential medium
Dpi	days post-infection
HA	hemagglutinin
HPAI	highly pathogenic avian influenza
Hpi	hours post-infection
IAV	influenza A virus
Ile	isoleucine
M1	**matrix**
MDCK	Madin-Darby canine kidney
MEM	Eagle's minimal essential medium
Met	methionine
MLD_{50}	50% mouse lethal doses
MOI	multiplicity of infection
mRNA	messenger ribonucleic acid
NA	neuraminidase

NCR	noncoding region
Nt	nucleotide
ORF	open reading frame
PFU	plaque-forming units
QT6	QT6 quail fibrosarcoma
RNP	ribonucleoprotein
SDS	sodium dodecyl sulfate
SDS-PAGE	sodium dodecyl sulfate polyacrylamide gel electrophoresis
Shimane	A/whistling swan/Shimane/499/83 (H5N3)
$TCID_{50}$	50% tissue culture infectious dose
vRNA	viral ribonucleic acid
WZ101	A/duck/Hokkaido/WZ101/2010 (H5N1)
WZ83	A/duck/Hokkaido/WZ83/2010 (H5N1)

Preface

Influenza A viruses (IAVs) are widely distributed in birds and mammals, including humans. The IAV genome consists of eight segments of negative-sense RNA, and is divided into subtypes on the basis of the combination of two surface glycoproteins, hemagglutinin (HA) and neuraminidase (NA), which are classified into each subtype based on antigenicity (H1-16 and N1-9, respectively) [1]. Epidemiological studies have revealed that wild water birds, particularly migratory ducks, are the natural reservoirs of IAVs [1]. All known IAV subtypes, except for H17N10 and H18N11 whose genomes were detected in bats [2,3], have been found in water birds [4,5].

Highly pathogenic avian influenza (HPAI) was first reported in Italy in 1878 as "fowl plague," a severe, rapidly spreading disease with high mortality in chickens [6]. This disease spread throughout Europe in the late 1800s and early 1900s via poultry exhibitions and shows, and it became endemic in domestic poultry until the 1930s [7]. In 1955, IAV was identified as the causative agent of fowl plague and shown to be related to other IAVs that infect mammals, including humans, pigs, and horses [7]. Since then, outbreaks of HPAI have been reported in many countries, resulting in devastating losses in poultry production worldwide.

In 1996, outbreaks of HPAI caused by H5N1 viruses occurred at a goose farm in China [8]. Moreover in 1997, outbreaks of HPAI caused by H5N1 viruses occurred at live bird markets in Hong Kong and human cases of H5N1 HPAI virus infection were subsequently reported [9,10]. Since then, H5N1 HPAI viruses have been circulating in poultry for more than a decade [11], leading to the death or euthanization of vast number of wild and domestic birds. In 2002, a large number of water birds, including

ducks, geese, and other birds, died because of H5N1 HPAI virus infection in Hong Kong [12]. Furthermore, in 2005, approximately 6,000 migratory water birds with H5N1 HPAI virus infection were found dead in Qinghai Lake, China [13]. Since then, many cases of fatal HPAI virus infection of wild birds, including ducks, have been reported in several countries. In addition to infection of avian species, it has been reported that H5N1 HPAI viruses are occasionally transmitted to humans and cause severe pneumonia with high case fatality rates [14]. Since the transmission of this virus to humans with a fatal outcome was first reported in 1997, 862 human cases, with 455 deaths, have been reported (as of 14 December in 2015, http://apps.who.int/iris/bitstream/10665/69373/1/WHO_PSM_PAR_2006.6_eng.pdf and http://www.who.int/influenza/human_animal_interface/EN_GIP_20151214cumulativeNumberH5N1cases.pdf?ua=1).

It is known that HPAI viruses evolve directly from low-pathogenic H5 and H7 viruses maintained in natural reservoirs [15-18]. Low-pathogenic IAVs contain a single arginine residue at the HA cleavage site, which is cleaved only by trypsin-like proteases and thus produce localized infection of the respiratory and/or intestinal tracts, causing asymptomatic or mild infection. After introduction into domestic poultry, low-pathogenic viruses often acquire multiple basic amino acids at the HA cleavage site, which is recognized by ubiquitous proteases such as furin and PC6 [19], thereby rendering these viruses capable of causing fatal systematic infection in terrestrial poultry. The polybasic HA cleavage site is known to be generated by multiple nucleotide insertions/substitutions to create codons for basic amino acids [17,20-22] or by recombination with cellular or viral RNA (vRNA) [23-25]. Although the polybasic HA cleavage site is considered to be the primary marker of HPAI viruses [16,26], it remains poorly understood why the

acquisition of the polybasic HA cleavage site is restricted to only H5 and H7 subtypes and how multiple nucleotide insertions/substitutions occur to create codons for basic amino acids.

In addition to the polybasic HA cleavage site, several molecular determinants of HPAI virus pathogenicity have been identified. Some amino acid residues in the polymerase subunits were shown to affect polymerase activity and to be important for the pathogenicity and host range of H5N1 HPAI viruses [27-30]. Deletions in the NA protein stalk region have been observed in many HPAI viruses [15,31,32]. Certain amino acids or regions of the NS1 protein have been reported to play a key role in the ability of H5N1 viruses to undermine the antiviral immune response of the host cells and to be critical for the pathogenicity of H5N1 viruses in mice [33-35]. In addition, other viral proteins have been reported to participate in the pathogenicity of H5N1 viruses [36-39]. However, in spite of extensive investigations, the genetic basis and mechanisms underlying the high pathogenicity of H5N1 HPAI viruses are not completely understood.

The present thesis consists of two chapters. In chapter I, it was shown that the amino acid at position 43 of the matrix (M1) protein, previously not identified as a molecular determinant of virulence of IAVs, could be a critical factor contributing to the high pathogenicity of H5N1 HPAI viruses in both avian and mammalian species. In chapter II, it is demonstrated that consecutive adenine residues and an enlarged stem-loop structure of the vRNA structure accelerate nontemplate nucleotide insertions and, a genetic basis for the acquisition of basic amino acid residues at the cleavage site of HPAI virus HA is discussed.

Chapter I

A Single Amino Acid in the M1 Protein Responsible for the Different Pathogenic Potentials of H5N1 Highly Pathogenic Avian Influenza Virus Strains

Introduction

The polybasic HA cleavage site is recognized by ubiquitous protease, and makes HPAI virus capable of causing systematic infection with fatal outcomes in terrestrial poultry. This mechanism plausibly explains the high lethality of HPAI viruses in chickens but not in mice [40]. Interestingly, HPAI viruses are, in general, known to show no or only mild pathogenicity for ducks although some H5N1 HPAI virus strains have been reported to kill them [12,41]. Thus, other factors in addition to the presence of multiple basic amino acids at the cleavage site of the HA should contribute to the pathogenicity of HPAI viruses for some hosts (e.g., mice and ducks) [30].

In 2010-2011, multiple outbreaks of H5N1 HPAI occurred in various parts of Japan [42]. In the same year, before those outbreaks, two strains of H5N1 HPAI viruses, A/duck/Hokkaido/WZ83/2010 (H5N1) (WZ83) and A/duck/Hokkaido/WZ101/2010 (H5N1) (WZ101), were isolated from fecal samples of apparently healthy migratory ducks arriving at the northernmost stopover site of the birds in Japan [43]. WZ83 and WZ101 are almost identical genetically and belong to the same clade, which contains several viruses detected over the whole of Japan and Korea [42]. In this study, it was found that WZ101 showed higher pathogenicity than WZ83 for chickens, ducks, and mice, despite the high genetic identity between these strains. To determine the molecular basis for the difference in pathogenicity between WZ83 and WZ101, we

generated reassortant viruses using a plasmid-based reverse genetics system, and found that the amino acid at position 43 of the M1 protein, previously not identified as a molecular determinant of virulence of IAVs, was the major contributor to the higher pathogenicity of WZ101 in both avian and mammalian species.

Materials and Methods

Viruses and cells

Influenza virus strains WZ83 and WZ101 were isolated from fecal samples of healthy migratory ducks arriving at Lake Ohnuma, Wakkanai, Hokkaido, en route south from their nesting areas in Siberia [43]. After isolated, these viruses were passaged once in 10-day-old embryonated chicken eggs at 35°C and stored at -80°C until use. Chicken and duck embryo fibroblasts (CEF and DEF, respectively) were prepared from 10-day-old chicken embryos and 13-day-old duck embryos, respectively, as previously described [44,45] with slight modification. Madin-Darby canine kidney (MDCK) cells [46], CEF, and DEF were grown in Dulbecco's minimal essential medium (DMEM) supplemented with 10% calf serum, 100 U/ml penicillin, and 0.1 mg/ml streptomycin. Human embryonic kidney 293T cells [47] were grown in DMEM supplemented with 10% fetal calf serum and antibiotics as described above. All cells were incubated at 37°C in a 5% CO_2 atmosphere unless otherwise indicated.

Construction of plasmids

vRNAs of WZ83 and WZ101 were extracted from infectious allantoic fluid using a QIAamp Viral RNA Mini Kit (Qiagen , Hilden, Germany) and reverse transcribed with Moloney murine leukemia virus reverse transcriptase (Invitrogen , Carlsbad, USA) using the uni12 primer (5'-AGCAAAAGCAGG) [48]. Then, for the expression of vRNAs, complementary DNAs (cDNAs) of WZ83 and WZ101 gene segments were cloned into the pHH21 vector, which contains the human RNA polymerase I promoter and the mouse RNA polymerase I terminator separated by the *Bsm*BI sites [49]. For the viral protein expression, the cDNAs encoding the PB2, PB1, PA, and NP genes of WZ83 and WZ101

were cloned into the multiple-cloning site of the eukaryotic expression vector pCAGGS/MCS (controlled by the chicken β-actin promoter) [50]. All of the plasmids constructed were sequenced to confirm the absence of unexpected mutations.

Generation of viruses from plasmids

Wild-type rgWZ83 and rgWZ101 and their reassortant viruses (rgWZ-83PB1/101M; WZ83 whose M gene was replaced with that of WZ101 and rgWZ-83M/101PB1; WZ101 whose M gene was replaced with that of WZ83) (Fig. 1) were generated by reverse genetics as described previously [49] with slight modification. Briefly, 293T cells were transfected with 1 μg of each of the 12 plasmids (8 plasmids for vRNA expression and 4 plasmids for viral polymerase and NP protein expression) encoding WZ83 and WZ101 genes using TransIT-LT1 (Mirus Bio, Madison, USA) according to the manufacturer's protocol. Forty-eight hours after transfection, the supernatants of transfected 293T cells were collected, diluted at 1:10, and transferred to confluent monolayers of MDCK cells. Rescued viruses were propagated in MDCK cells and titers were determined as plaque-forming units (PFU) using MDCK cells and a 50% tissue culture infectious dose ($TCID_{50}$) using CEF, DEF, and MDCK cells. The genomes of the rescued viruses were sequenced to confirm the absence of unexpected mutations.

Experimental infection of chickens, ducks, and mice

All experimental protocols were reviewed and approved by the Hokkaido University Animal Care and Use Committee (Approval number: 08-0234, 13-0138). Four-week-old chickens (Boris Brown), 2-week-old domestic ducks (Cherry Valley, kindly provided by Takikawa Shinseien, Hokkaido, Japan), and 7-week-old female mice (BALB/c) were used

to assess the pathogenicity of the viruses. Eight chickens in each group were intravenously infected with each virus (10^6 PFU/bird) and monitored clinically at 8-hour intervals over the period of 6 days. Six chickens in each group were intranasally infected with each virus (10^6 PFU/bird) and monitored clinically at 24-hour intervals over the period of 14 days. Five ducks in each group were infected intranasally with each virus (10^6 PFU/bird) and monitored clinically at 12-hour intervals over the period of 14 days. Clinical signs of infected ducks were evaluated and scored daily on the scale of 0-3 (0 = healthy; 1 = mild ill; 2 = severe ill; 3 = dead) during the observation period. Birds exhibiting severe disease signs (i.e. severe neurological symptoms or paralysis) were euthanized with isoflurane and death was recorded as occurring the next day. Three mice in each group were intranasally infected with each virus (10, 10^2, 10^3, and 10^4 PFU/head), and their body weights and survival (fatality) rates were monitored at 24-hour intervals over the period of 14 days. Mice with body weight loss of more than 25% of their original body weight were euthanized with isoflurane and death was recorded as occurring the next day. These animal experiments were carried out in the biosafety level 3 facility at the Hokkaido University Research Center for Zoonosis Control, Japan. Statistical significance of survival time for chickens that died during the experimental period and the mean clinical score of individual ducks were calculated using student's *t*-test with Bonferroni correction.

Growth kinetics of viruses in DEF, CEF, and MDCK cells

Cultured DEF, CEF, and MDCK cells were infected with each virus at the multiplicity of infection (MOI) of 0.001. After adsorption for 1 hour, the inoculum was removed and cells were washed and overlaid with Eagle's minimal essential medium (MEM)

containing bovine serum albumin (0.3%), penicillin (100 U/ml), and streptomycin (0.1 mg/ml). DEF, CEF, and MDCK cells were incubated at 40°C or 35°C, and the culture supernatants were collected at various time points. The titers of viruses released into cell culture supernatants were determined by plaque assays in MDCK cells.

Cycloheximide treatment and detection of M1 protein in infected CEF

CEF were infected with each virus at the MOI of 2 and incubated for 6 hours. Then the culture medium was replaced by MEM supplemented with bovine serum albumin (0.3%), penicillin (100 U/ml), and streptomycin (0.1 mg/ml) containing cycloheximide (CHX) (100 μg/ml) or ethanol (solvent for CHX) and the incubation was continued for further 6 hours at 37°C. Cells were lysed in sodium dodecyl sulfate (SDS) buffer containing 2-mercaptoethanol (2-ME), and the M1 protein and β-actin in whole cell lysate was detected as described below. Samples were heated for 5 minutes at 98°C and analyzed by 10% SDS-polyacrylamide gel electrophoresis (SDS-PAGE). After electrophoresis, separated proteins were blotted onto a polyvinylidene difluoride membrane (Merck Millipore, Guyancourt, France). Mouse monoclonal antibodies against the M1 protein (APH6-23-1-6) [51] and β-actin (Abcam, Cambridge, USA) were used as primary antibodies to detect the M1 and β-actin, respectively. The bound antibodies were detected with peroxidase-conjugated goat anti-mouse IgG (H+L) (Jackson ImmunoResearch, West Grove, USA), followed by visualization with Immobilon Western (Merck Millipore, Guyancourt, France). Band intensities of the M1 protein were analyzed with a VersaDocTM Imaging System (Bio-Rad, Hercules, USA) and Image LabTM software (Bio-Rad, Hercules, USA).

Results

Characterization of WZ83 and WZ101

It was first first found that chickens infected intravenously with WZ83 or WZ101 uniformly showed loss of appetite, lethargy, subcutaneous hemorrhages in the legs, edema of the face and legs, and paralysis. However, it was noted that WZ101 killed the chickens more rapidly than WZ83; chickens infected with WZ83 died at 72-128 hours post-infection (hpi) whereas those infected with WZ101 died at 40-56 hpi (Fig. 2A) (p<0.001 for the comparison of the mean death time). Then all the RNA segments were sequenced and it was demonstrated that WZ83 and WZ101 were almost identical and differed by only two amino acids in the M1 and PB1 proteins, the primary products of the M and PB1 RNA segments. WZ83 and WZ101 have isoleucine (Ile) and methionine (Met) at amino acid position 43 of M1, and Ile and Met at amino acid position 317 of PB1, respectively. No difference was found in the M2 and PB1-F2 proteins, which were also expressed by the respective gene segments.

Pathogenicities of rgWZ83, rgWZ101, rgWZ-83PB1/101M, and rgWZ-83M/101PB1 in chickens

To investigate the genetic basis of the difference in pathogenicity between WZ83 and WZ101, the author established a reverse genetics system for these viruses and rescued wild-type and their reassortant viruses (Fig. 1). Intravenous inoculation of these viruses caused similar clinical symptoms and 100% mortality in 4-week-old chickens. Consistent with the difference between the original strains (Fig. 2A), rgWZ101 killed chickens more rapidly than rgWZ83 (i.e., while chickens infected with rgWZ83 died at 64-112 hpi, those

infected with rgWZ101 died at 40-64 hpi) (p<0.01 for the comparison of the mean death time between rgWZ83 and rgWZ101). Interestingly, the pathogenicities of rgWZ-83PB1/101M and rgWZ-83M/101PB1 were similar to those of rgWZ101 and rgWZ83, respectively (i.e., chickens infected with rgWZ-83PB1/101M died at 40-64 hpi whereas those infected with rgWZ-83M/101PB1 died at 64-104 hpi) (Fig. 2B) (p<0.01 for the comparison of the mean death time between rgWZ83 and rgWZ-83PB1/101M and between rgWZ101 and rgWZ-83M/101PB1). The pathogenicities of these viruses were also investigated in chickens infected intranasally (Fig. 2C). It was found that all 4 viruses were highly lethal in intranasally infected chickens, and there was an appreciable difference between rgWZ83 and rgWZ101, as was the case with intravenously infected chickens (p<0.001 for the comparison of the mean death time between rgWZ83 and rgWZ101). Chickens infected with rgWZ101 or rgWZ-83PB1/101M died at 3-7 days post-infection (dpi), whereas chickens infected with rgWZ83 or rgWZ-83M/101PB1 died at 5-8 dpi except for one rgWZ83-infected chicken surviving during the 14-day observation period (Fig. 2C) (p<0.01 for the comparison of the mean death time between rgWZ83 and rgWZ-83PB1/101M and between rgWZ101 and rgWZ-83M/101PB1). These results indicated that the M gene of WZ101 contributed to the higher pathogenicity of rgWZ101 in chickens.

Pathogenicities of rgWZ83, rgWZ101, rgWZ-83PB1/101M, and rgWZ-83M/101PB1 in ducks

Then pathogenicities of all 4 rescued viruses in ducks were compared (Fig. 2D). All ducks infected with rgWZ83 survived and showed no or only mild clinical symptoms (e.g. somnolentia and lethargy) during the 14-day observation period. In contrast, ducks

infected with rgWZ101 showed loss of appetite, lethargy, torticollis, uncontrollable shaking, marked loss of balance, and paralysis, and 4 of the 5 ducks died at 5-7 dpi ($p<0.01$ for the comparison of the mean clinical score between rgWZ83 and rgWZ101). Unlike rgWZ83, rgWZ-83PB1/101M caused severe clinical symptoms in all ducks and killed 3 of the 5 infected ducks at 7-10 dpi ($p<0.01$ for the comparison of the mean clinical score between rgWZ83 and rgWZ-83PB1/101M). Interestingly, rgWZ-83M/101PB1 did not kill any ducks and caused no or only mild clinical symptoms, as was the case with rgWZ83 ($p<0.01$ for the comparison of the mean clinical score between rgWZ101 and rgWZ-83M/101PB1). These results indicated that the single amino acid difference in the M1 protein was a critical factor associated with the lethality of WZ101 in ducks.

Pathogenicities of rgWZ83, rgWZ101, rgWZ-83PB1/101M, and rgWZ-83M/101PB1 in mice

Furthermore, the pathogenicities of these viruses in mice were compared (Fig. 2E). Four infectious doses (10, 10^2, 10^3, or 10^4 PFU) of each virus were inoculated intranasally into mice (three mice for each dose). It was found that rgWZ101 killed all the mice, even at the lowest dose tested (10 PFU), whereas a much higher dose (10^4 PFU) was required for rgWZ83 to kill all three mice. Both rgWZ-83PB1/101M and rgWZ-83M/101PB1 were lethal for mice at the highest dose (10^4 PFU) but not at the lowest dose (10 PFU). Interestingly, at the moderate dose (10^2 PFU), rgWZ-83PB1/101M was lethal and killed all three mice, whereas rgWZ-83M/101PB1 killed no mice. The 50% mouse lethal doses (MLD_{50}) of rgWZ83, rgWZ101, rgWZ-83PB1/101M, and rgWZ-83M/101PB1 were 10^3, <10, 3.16×10, and 1.78×10^3 PFU, respectively. These results suggested that the single amino acid difference in the PB1 protein, in addition to the M1 protein, was also involved

in the higher pathogenicity of WZ101 in mice.

Growth kinetics of rgWZ83, rgWZ101, rgWZ-83M/101PB1, and rgWZ-83PB1/101M in CEF, DEF, and MDCK cells

To compare the *in vitro* replication capacities of the viruses, their growth kinetics were tested in CEF, DEF, and MDCK cells at 40°C and 35°C. It was found that rgWZ101 replicated more efficiently than rgWZ83 in CEF and DEF at 40°C, as indicated by approximately 10-fold higher titers than those of rgWZ83 at 48 and 72 hpi (Fig. 3A and B). The growth kinetics of rgWZ-83PB1/101M and rgWZ-83M/101PB1 were similar to those of rgWZ101 and rgWZ83 in CEF and DEF, respectively (Fig. 3A and B). Interestingly, the difference was less significant when the viruses were grown in CEF and DEF at 35°C (Fig. 3D and E). In MDCK cells, rgWZ101 and rgWZ-83PB1/101M showed higher titers than rgWZ83 and rgWZ-83M/101PB1 at several time points when grown at 40°C (Fig. 3C). However, unlike the growth kinetics in CEF and DEF, overall differences between the viruses were limited and not clear in MDCK cells.

Difference in the stability of the M1 proteins in cultured cells

Since the M1 protein was shown to be important for the difference in the pathogenicity and replication capacity between WZ83 and WZ101, the author then sought to find the difference in biological properties of the M1 protein among the strains. The stability of the M1 protein was focused on since the author hypothesized that it might be involved in viral pathogenesis. rgWZ83- and rgWZ101-infected CEF were incubated for 6 hours followed by the incubation with CHX for 6 more hours, and the amounts of the M1 protein were compared (Fig. 4A and B). Without CHX treatment, similar amounts of

the M1 protein were detected in CEF infected with rgWZ83 and rgWZ101. As expected, reduced amounts of the M1 protein of rgWZ83 and rgWZ101 were detected in infected CEF incubated with CHX. Interestingly, it was found that the amount of the rgWZ101 M1 protein was significantly lower than that of the rgWZ83 M1 protein in CHX-treated CEF. These results suggested that the WZ101 M1 protein was more unstable and degraded more rapidly in CEF than the WZ83 M1 protein.

Discussion

In this study, it was found that two H5N1 HPAI virus strains isolated in Japan, WZ83 and WZ101, were genetically almost identical but had different pathogenicities. It was demonstrated that rgWZ101 had higher pathogenicity than rgWZ83 in chickens, ducks, and mice and that the amino acid at position 43 in the M1 protein, not reported previously to be associated with virulence of IAVs, was responsible for the higher pathogenicity of WZ101. It was further demonstrated that this amino acid affected the *in vitro* replication capacity of WZ83 and WZ101 and the stability of the M1 protein in infected cells.

Based on sequences obtained from the NCBI Influenza Virus Resource Database, the amino acid at position 43 of the M1 protein is highly conserved among IAVs (i.e., 1194 of 1201 viruses isolated from avian species and 2648 of 2662 viruses isolated from all hosts have Met at this position of the M1 protein). In 2010 and 2011, many strains of the H5N1 HPAI viruses closely related to WZ83 and WZ101 were isolated not only in Japan but also in China, Mongolia, Russia, and Korea. However, all of these viruses except for WZ83 have Met at amino acid position 43 of the M1 protein. These observations suggest that Met at amino acid position 43 of the M1 protein is important for the viral life cycle and/or not exposed to selection pressure. Importantly, however, WZ83 still retained high pathogenicity in chickens and high replication capacity *in vitro*, indicating that the substitution at this position might not affect the fundamental functions of the M1 protein.

The M1 protein is a multifunctional protein playing many essential roles throughout the viral replication cycle. It forms the major structural component of influenza virus

particles, plays an essential role in viral assembly associated with influenza virus ribonucleoprotein (RNP) and RNA [52-56], functions in transcription inhibition [57], and controls RNP nuclear import and export [58-62]. However, little has been reported about the direct contribution of the M1 protein to the pathogenicity of H5N1 HPAI viruses. Two amino acid residues at positions 30 and 215 of the M1 protein were reported to be important for the pathogenicity of H5N1 HPAI viruses in mice [38]. While these 2 amino acids are located in the second helix and C-terminal domain of the M1 protein, respectively, amino acid position 43, which is responsible for the difference in the pathogenicity between WZ83 and WZ101, is located in the N-terminal domain and fold into the third helix of the M1 protein [63,64]. The amino acid substitution at position 41 of the M1 protein has been reported to be associated with increased replication and virulence of human influenza viruses in mice, suggesting a role in host adaptation [65]. This amino acid residue was also implicated in determining the virion morphology (i.e., filamentous or spherical) of influenza viruses [66,67], while both rgWZ83 and rgWZ101 virions were spherical (data not shown). These observations suggested the different contributions of these amino acids to the pathogenicities of H5N1 HPAI viruses in different animals.

It was also noted that the difference in growth kinetics experiments between WZ83 and WZ101 was most apparent in avian cells at the higher temperature. In general, avian influenza viruses replicate at higher temperatures than human influenza viruses, most likely due to higher temperature of avian species compared to mammals. It was shown that *in vitro* replication capacity at higher temperature (41°C) was correlated with the pathogenicity of some HAPI virus strains in chickens [68]. Therefore, efficient replication of WZ101 at higher temperature is likely linked to its increased

pathogenicity particularly in chickens and ducks. It was also suggested that the M gene segment of a live attenuated human influenza vaccine strain affected temperature sensitivity of the virus [69]. Although detailed mechanisms are not clear, it is assumed that amino acid position 43 is involved in the thermal stability of the WZ101 M1 protein which might contribute to the pathogenicity.

It has been suggested that difference in viral protein degradation in infected cells could affect the pathogenicity of the rabies virus [70]. A rabies virus strain with a higher degradation rate of its G protein induced less apoptosis in infected neuronal cells and had a 50% higher pathogenicity index for mice than a variant strain with a lower degradation rate of the G protein [70]. It is known that the M1 protein of IAVs mediates the activation of caspase, which plays essential roles in inducing apoptosis both in viral infected and M1-expressing cells [71]. Although the transient expression of WZ83 and WZ101 M1 proteins in 293T and Hela cells did not affect the caspase activity (data not shown), these data suggested that the WZ101 M1 protein was more unstable and degraded more rapidly in virus-infected CEF than the WZ83 M1 protein. Thus, it might be possible that rapid degradation of the WZ101 M1 protein results in weaker anti-viral host responses due to reduced apoptosis and/or antigen presentation of infected cells.

In summary, it was demonstrated that the amino acid at position 43 of the M1 protein could be a critical factor contributing to high pathogenicities of H5N1 HPAI viruses for both avian and mammalian species, although the underlying mechanisms remain to be determined. It is noteworthy that the amino acid difference at this position particularly affected viral pathogenicity in ducks. These data underscore the need for continued global monitoring of H5N1 HPAI viruses for early detection of HPAI viruses with reduced virulence to ducks due to the substitution at this amino acid position,

enabling us to take preemptive measures to minimize the risk of their transmission to domestic poultry. It is also important to investigate whether such viruses are naturally selected and become predominant in wild duck populations.

Summary

Two HPAI virus strains, WZ83 and WZ101, which were isolated from wild ducks in Japan, were found to be genetically similar, with only two amino acid differences in their M1 and PB1 proteins at positions 43 and 317, respectively. It was found that both WZ83 and WZ101 caused lethal infection in chickens but WZ101 killed them more rapidly than WZ83. Interestingly, ducks experimentally infected with WZ83 showed no or only mild clinical symptoms, whereas WZ101 was highly lethal. Then reassortants between these viruses were generated and it was revealed that exchange of the M gene segment completely switched the pathogenic phenotype in both chickens and ducks, indicating that the difference in the pathogenicity for these avian species between WZ83 and WZ101 was determined by only a single amino acid in the M1 protein. It was also found that WZ101 showed higher pathogenicity than WZ83 in mice and that WZ83, whose M gene was replaced with that of WZ101, showed higher pathogenicity than wild-type WZ83, although this reassortant virus was not fully pathogenic compared to wild-type WZ101. These results suggest that the amino acid at position 43 of the M1 protein is one of the factors contributing to the pathogenicity of H5N1 HPAI viruses in both avian and mammalian hosts.

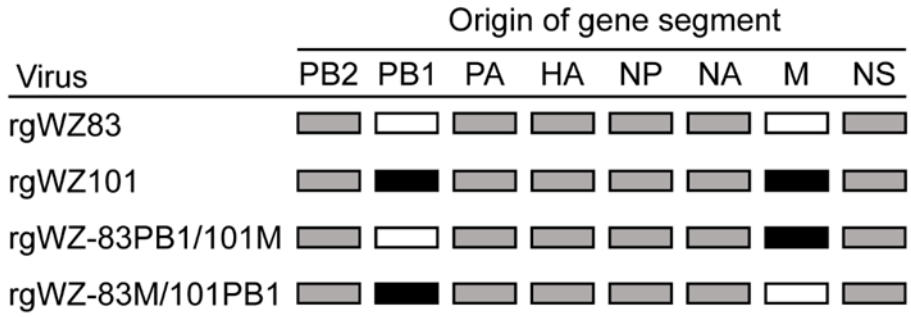

Fig. 1. Viruses used in this study.

Wild-type (rgWZ83 and rgWZ101) and reassortant viruses (rgWZ-83PB1/101M; WZ83 whose M gene was replaced with that of WZ101 and rgWZ-83M/101PB1; WZ101 whose M gene was replaced with that of WZ83) were generated as described in the Materials and Methods section.

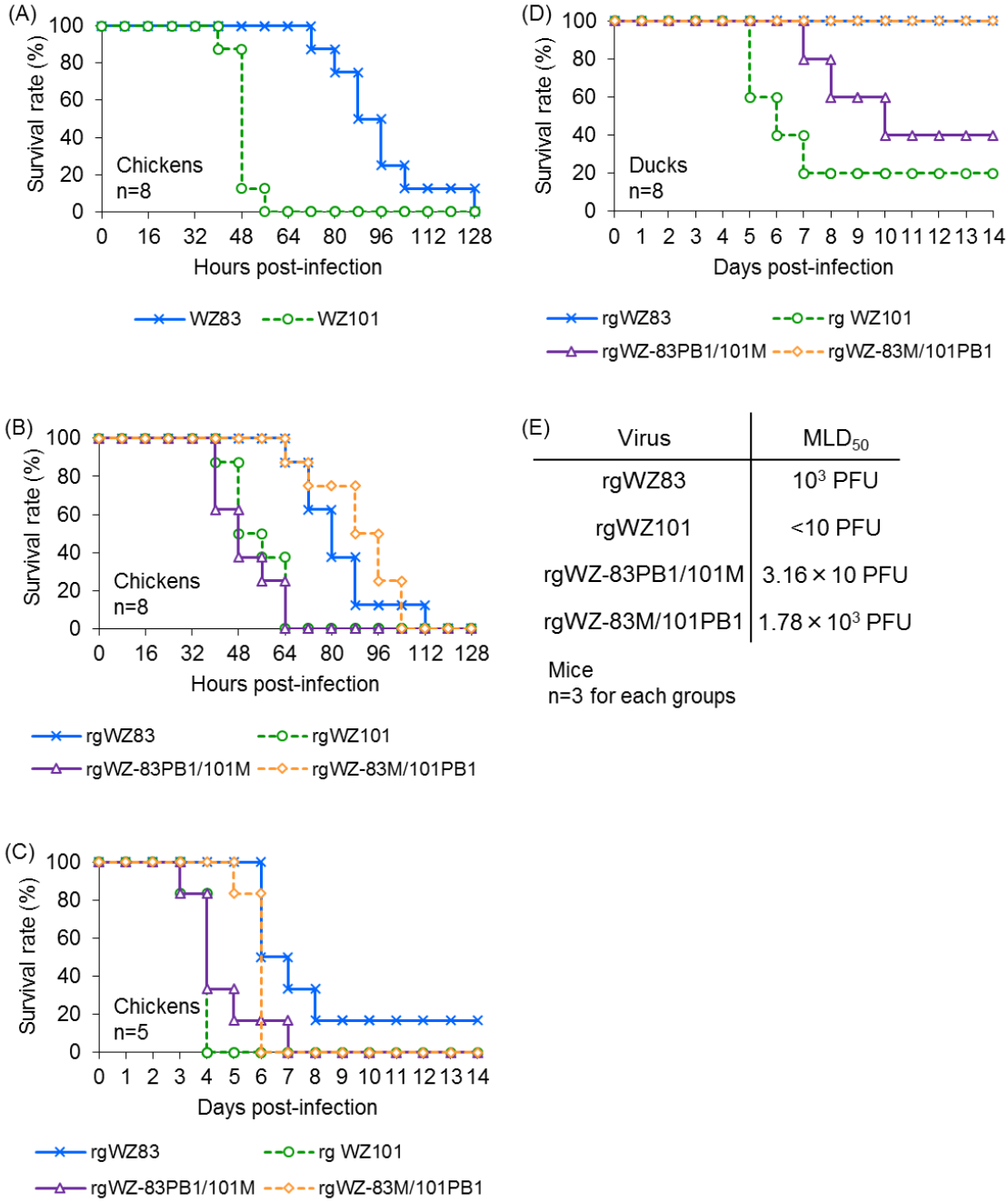

(E)

Virus	MLD_{50}
rgWZ83	10^3 PFU
rgWZ101	<10 PFU
rgWZ-83PB1/101M	3.16×10 PFU
rgWZ-83M/101PB1	1.78×10^3 PFU

Mice
n=3 for each groups

Fig. 2. Pathogenicities of H5N1 HPAI viruses for chickens, ducks, and mice.

Eight chickens of each group were intravenously infected with 10^6 PFU of 2 original isolates (WZ83 and WZ101) (A). Eight chickens of each group were intravenously infected with 10^6 PFU of plasmid-derived viruses (rgWZ83, rgWZ101, rgWZ-83PB1/101M, and rgWZ-83M/101PB1) and observed for clinical symptoms every 8 hours (B). Six chickens of each group were intranasally infected with 10^6 PFU of each

virus and observed for clinical symptoms every 24 hours (C). Five ducks of each group were intranasally infected with 10^6 PFU of rgWZ83, rgWZ101, rgWZ-83PB1/101M, or rgWZ-83M/101PB1 and observed for clinical symptoms every 12 hours (D). Three mice of each group were intranasally infected with one of 4 infectious doses (10, 10^2, 10^3, or 10^4 PFU) of each virus, and MLD50 was calculated (E).

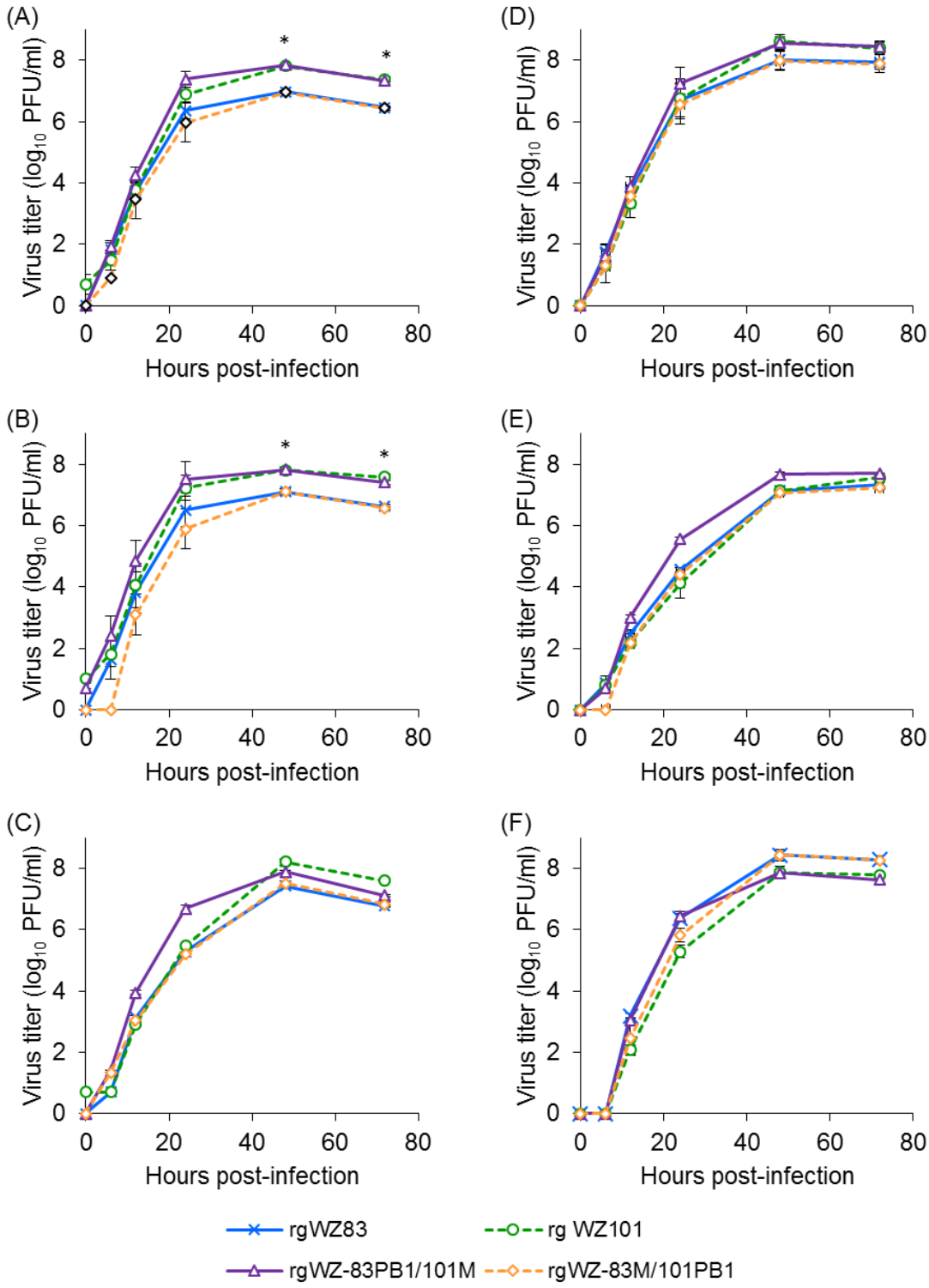

Fig. 3. Comparison of growth kinetics of H5N1 HPAI viruses in cultured cells.
Growth kinetics of rgWZ83, rgWZ101, rgWZ-83PB1/101M, and rgWZ-83M/101PB1 in CEF (A and D), DEF (B and E), and MDCK cells (C and F) at 40°C (A, B, and C) and

35°C (D, E, and F) were compared. The results are presented as the averages and standard deviations of three independent experiments. Statistical significance was calculated using student's *t*-test for the comparison between rgWZ83 and rgWZ101, rgWZ83 and rgWZ-83PB1/101M, rgWZ101 and rgWZ-83M/101PB1, and rgWZ-83PB1/101M and rgWZ-83M/101PB1 with Bonferroni correction for time points 48 and 72 hpi (*p<0.01 for all comparisons).

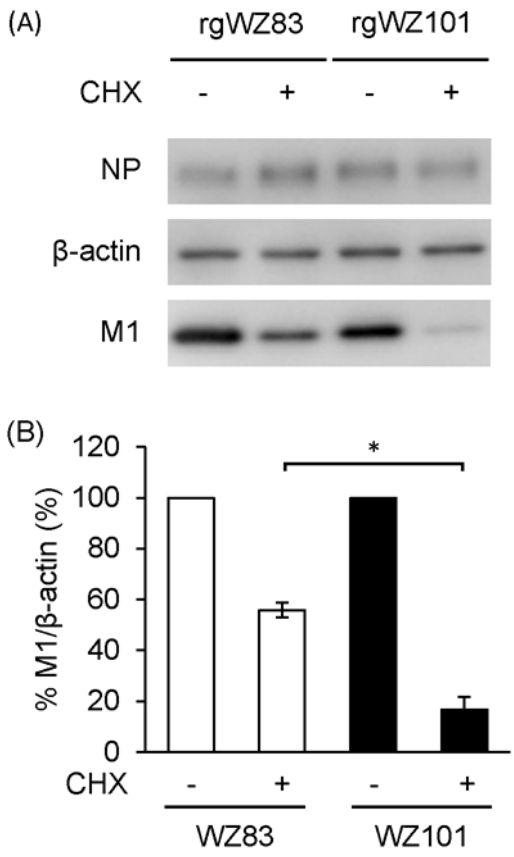

Fig. 4. Stability of the M1 protein in cultured cells.

CEF were infected with rgWZ83 and rgWZ101 and incubated for 6 hours at 37°C. Then cells were treated with CXH and further incubated for 6 hours. The amount of the M1 protein was measured by western blotting and β-actin was used as a loading control. Representative data of three independent experiments are shown (A). Relative percentages of band intensities of the M1 protein are presented as the averages and standard deviations of three independent experiments (B). Statistical significance was calculated using student's *t*-test (**p*<0.01).

Chapter II

A genetic basis for the acquisition of basic amino acid residues at the cleavage site of influenza virus hemagglutinin

Introduction

Most outbreaks of HPAI are caused only by IAVs of the H5 and H7 subtypes. However, it was reported that an H6 virus with an artificially introduced polybasic HA cleavage site acquired high HA cleavability without trypsin and had a typical HPAI phenotype in experimentally infected chickens [72]. In addition, an H9 virus acquires intravenous pathogenicity in chickens via the introduction of a pair of dibasic amino acid residues at the HA cleavage site and consecutive passages in chickens [73]. Furthermore, some other HA subtypes also support a highly pathogenic phenotype in the genetic background of an HAPI virus after artificial introduction of the polybasic HA cleavage site [74]. These studies strongly suggest that the restriction of naturally occurring insertions or substitutions to get multiple basic amino acids into the cleavage sites of H5 and H7 HAs is likely due to the unique genetic predisposition of these HA subtypes, not a structural or functional limitation of the HA molecule.

In this study, the author focused on the A/whistling swan/Shimane/499/83 (H5N3) (Shimane) strain, which was originally isolated as a low-pathogenic strain and shown to become highly pathogenic after passaging through experimentally infected chickens [21]. During serial passage through chickens, Shimane first underwent two point mutations at nucleotide positions 1050 (C to A) and 1046 (G to A) in the vRNA sequence encoding the HA cleavage site and then acquired a series of basic amino acids, R-R-K-K-R, via the insertion of a codon for an arginine residue at the HA cleavage site

[21] (Fig. 5). It was found that the primary point mutations in Shimane genomic RNA enlarged the stem-loop structure of the predicted secondary structure of the vRNA region encoding the HA cleavage site and increased the frequency of nucleotide insertions, which might accelerate the acquisition of additional codons for basic amino acids at the HA cleavage site. It was further confirmed that nucleotide insertions into the predicted loop structure were indeed seen in vRNAs of Shimane virions. These data suggest that the vRNA sequence encoding the HA cleavage site of Shimane might have a key role in inducing viral polymerase slippage, resulting in increased frequency of nucleotide (adenine and guanine) insertions, which might contribute to creating the polybasic HA cleavage site.

Materials and methods

Viruses and cells

IAV Shimane strain was kindly provided by Dr. T. Ito, Tottori University. The virus was propagated in the allantoic cavities of 10-day-old embryonated chicken eggs at 35°C for 48 hours and stored at -80°C until use. MDCK cells [46] were grown in DMEM supplemented with 10% calf serum, 100 U/ml penicillin, and 0.1 mg/ml streptomycin. 293T cells [47] were grown in DMEM supplemented with 10% fetal calf serum and antibiotics as described above. QT6 quail fibrosarcoma (QT6) cells [75] were maintained in Kaighn's modification of Ham's F-12 medium supplemented with 5% calf serum and 10% tryptose phosphate broth. All cells were incubated at 37°C in a 5% CO_2 incubator.

Reporter Assay

The author used modified pHW72 plasmid [76] (pHW72-LUC-CKpolI) containing the chicken RNA polymerase I promoter, mouse RNA polymerase I terminator, PR8 HA segment-derived noncoding region (NCR), and firefly luciferase gene (Fig. 6A). The reporter plasmid was constructed by inserting 28, 29, or 30 polynucleotides (i.e., linkers) whose sequences were derived from those encoding amino acids around the HA cleavage site of Shimane (Fig. 6B), upstream of the firefly luciferase gene. This construct was flanked by PR8 HA-NCR at both the 5' and 3' ends (Fig. 6C). Eukaryotic expression plasmid pCAGGS/MCS (controlled by the chicken β-actin promoter) encoding the PR8 virus polymerases (PB2, PB1, and PA) and NP were kindly provided by Dr. Y. Kawaoka, University of Tokyo. Seventy percent-confluent QT6 cell

monolayers in 24-well tissue culture plates were transfected with 150 ng of pHW72-LUC-CKpolI plasmids with the respective linkers, 5ng of a pRL-TK Renilla luciferase transfection control reporter plasmid (Promega), and a mixture of PB2-, PB1-, PA-, and NP-expressing plasmids in quantities of 150 ng, 150 ng, 150 ng, and 300 ng, respectively, using FuGENE HD (Promega, Madison, USA) according to the manufacturer's protocol. At 24 hours post-transfection, luciferase (firefly and Renilla luciferase) activities of cell lysates were measured with a GloMax96 Microplate Luminometer (Promega, Madison, USA) using the Dual-Luciferase assay system (Promega, Madison, USA) according to the manufacturer's protocol. Firefly luciferase activities were standardized to the transfection control Renilla luciferase activities (i.e., firefly luciferase activities were divided by Renilla luciferase activities).

Prediction of RNA secondary structure

The Mfold program (http://unafold.rna.albany.edu/?q=mfold/rna-folding-form) [77] was used to predict the secondary structures of vRNA corresponding to the linker sequences.

Generation of infectious viruses from plasmids

The vRNA of Shimane was extracted from infectious allantoic fluids using a QIAamp Viral RNA Mini Kit (Qiagen, Hilden, Germany) and reverse-transcribed with Moloney murine leukemia virus reverse transcriptase (Invitrogen, Carlsbad, USA) using the uni12 primer (5'-AGCAAAAGCAGG) [48]. Then, for the expression of the Shimane vRNA, cDNA of the HA gene segment was cloned into the pHH21 plasmid, which contains the human RNA polymerase I promoter and the mouse RNA polymerase

I terminator separated by *Bsm*BI sites [49]. A reassortant virus between PR8 and Shimane (rgPR8/Shimane-HA; PR8 whose HA gene was replaced with that of Shimane) was generated by a reverse genetics system as described previously [49] with slight modification. Briefly, 293T cells were transfected with 1 μg of each of the 12 plasmids (8 pHH21-based plasmids for vRNA expression and 4 pCAGGS-based plasmids, described above, for viral polymerases and NP expression) encoding PR8 and Shimane genes using TransIT-LT1 (Mirus Bio) according to the manufacturer's protocol. Forty-eight hours after transfection, the supernatant of transfected 293T cells was collected, diluted 1:10, and transferred into confluent monolayers of MDCK cells. Rescued viruses were propagated in MDCK cells and titers were determined as PFU using MDCK cells and stored at -80°C until use.

Virus purification and RNA extraction

Cultured MDCK cells, maintained in MEM containing bovine serum albumin (0.3%), penicillin (100 U/ml), and streptomycin (0.1 mg/ml), were infected with rgPR8/Shimane-HA at the MOI of 0.001, incubated at 37°C for 48 hours, and then the infectious supernatant was collected. Virus particles were concentrated and purified by high-speed centrifugation (28,000 rpm for 2 hours at 4°C) of the supernatant through a 10-50% sucrose density gradient. RNAs were extracted from purified virus particles using TRIzol LS Reagent (Thermo Fisher Scientific, Waltham, USA) according to the manufacturer's protocol.

Library preparation and Illumina sequencing

Extracted vRNA (10 μg) was used for the synthesis of double-stranded cDNA of the partial HA gene containing the sequence encoding the HA cleavage site with a PrimeScript Double Strand cDNA Synthesis Kit (Takara, Kusatsu, Japan) using the HA gene specific primer (ShimaneHA963F; 5'-GTATGCCTTTCCACAATATTCATCC). The synthesized double-stranded cDNA (approximately 750 bp) was tagged with sequencing adapters with indexes by using a TruSeq DNA PCR-Free Sample Prep Kit (Illumina, San Diego, USA). The cDNA library was verified on a high sensitivity DNA chip on a Bioanalyzer (Agilent Technologies, Palo Alto, USA) and quantified with real-time PCR using an Illumina compatible kit and standards (KAPA Biosystems, Woburn, USA) before loading on the sequencing chip. Then the indexed library was sequenced using a MiSeq v3 600-cycle kit (Illumina) to perform 300-bp paired-end sequencing on a MiSeq instrument (Illumina), according to the manufacturer's instructions. After the sequencing run, reads with the same index sequences were grouped together.

Data analysis

CLC Genomic Workbench version 8.0.2 (NDCLC Bio, Aarhus, Denmark) was used to analyze and process the sequencing reads. First, the sequencing reads were trimmed from both sides using the modified Mott trimming algorithm to obtain a Q20 score, and all ambiguous bases were removed from the reads. The reads with a length below 100 bp were also removed. Next, the processed reads were aligned with the reference HA sequence (Shimane) determined by Sanger sequencing, using local alignment with the following settings: mismatch = −1, insertion/deletion = −1, length fraction = 1.0 and similarity fraction = 0.9. Nonspecific matches, defined as reads aligning to more than one position with an equally good score, were ignored. Then, the

basic variant detection tool in CLC was employed to identify variants using the following settings: neighborhood radius: 1, minimum neighborhood quality: 30, and minimum central quality: 30.

Results

Reporter gene expression resulting from nontemplate nucleotide insertions into the Shimane HA sequence

The reporter assay was established to quantitatively detect nucleotide insertions into the sequence encoding amino acids around the HA cleavage site of Shimane. In this assay, negative sense vRNA is transcribed from pHW72-LUC-CKpolI by RNA polymerase I of QT6 cells. Then messenger RNA (mRNA) and complementary RNA (cRNA) are transcribed from this vRNA template by PR8 RNA polymerases and NP, which are provided by the cotransfected expression plasmids (i.e., pCAGGS). The transcripts from the pHW72-LUC-CKpolI plasmids contain 5' NCR of HA followed by a start codon, 28-30 polynucleotide linkers, the firefly luciferase reporter gene, and the 3' NCR of HA (Fig. 6B and C). The constructs containing 28 or 29 polynucleotide linkers produce mRNAs that are not in-frame with the open reading frame (ORF) of the reporter gene. Therefore, the firefly luciferase is expected to be expressed when nucleotides are inserted into the linker region of mRNA and/or cRNA to make the linker sequence in-frame with the ORF of the reporter gene.

To evaluate this system, the author first tested pHW72-LUC-CKpolI plasmids containing the linkers (Linker28, Linker29, and Linker30), all of which had the sequence derived from the Shimane gene encoding amino acids around the HA cleavage site (Fig. 5 and Fig. 6B). QT6 cells were transfected with these plasmids and luciferase activities of cell lysates were measured (Fig. 7A). As expected, a high level of luciferase activity was detected in the cells transfected with the construct with Linker30, having the sequence in-frame with the ORF of the reporter gene. Interestingly, it was found that the

pHW72-LUC-CKpolI plasmid containing Linker28 or Linker29 also expressed slightly but significantly higher levels of luciferase than the empty plasmid. Significantly higher luciferase expression was observed in QT6 cells transfected with the plasmid containing Linker29 than with Linker28. These results suggested that nontemplate nucleotide insertions into these linker regions occurred during the synthesis of mRNA, cRNA, and/or vRNA.

Accelerated nucleotide insertions in the presence of consecutive adenine residues

Then it was hypothesized that a stretch of adenine residues in this region might affect the frequency of nucleotide insertions, as has been suggested with the RNA editing mechanism of some RNA viruses [78-82]. Runs of adenines are present in the RNA editing site of ebolaviruses [79] and paramyxoviruses [78] where the virus polymerase inserts nontemplate nucleotide(s) during mRNA synthesis to create alternative reading frames. The increase in the number of adenine residues in the editing site of paramyxoviruses enhances the frequency of additional nucleotide insertion(s) at the editing site [78]. In addition to viral polymerases, it has been reported that transcriptional slippage by *Escherichia coli* RNA polymerase during RNA elongation at runs of 10 or more adenines or thymines results in the addition of nontemplate uracil or adenine residues, leading to the restoration of the normal reading frame from out-of-frame lacZ constructs [83]. Thus, to confirm the hypothesis, the author constructed another pHW72-LUC-CKpolI plasmid with a modified version of Linker29 including runs of 10 adenines with G- or C-to-A substitutions (linker29-10A) (Fig. 6B) and compared the luciferase activities. Much higher levels of luciferase expression was found in QT6 cells transfected with this plasmid (Fig. 7A), most likely due to increased

frequency of the nucleotide insertion by viral polymerase slippage.

Next the author tested the effect of the two nucleotide substitutions (C or G to A), that had actually occurred in the Shimane HA gene prior to the nucleotide insertion to create a codon for an arginine residue at the HA cleavage site [21]. The author constructed pHW72-LUC-CKpolI plasmids with Linker29-24a and Linker29-24a2b having the sequences of strains 24a and 24a2b, which had 6 and 8 consecutive adenines in the corresponding sequences, respectively (Fig. 5 and Fig. 6B). It was found that the amount of luciferase expression by pHW72-LUC-CKpolI containing a single substitution (Linker29-24a) was similar to that by the plasmid with Linker29 but, interestingly, the additional substitution (Linker29-24a2b) significantly enhanced the luciferase expression (Fig. 7B). These results suggested that these two nucleotide substitutions resulting in the presence of 8 adenine residues accelerated the nucleotide insertion into the linker sequence.

Nontemplate nucleotide insertions found in the vRNA of purified virions

To confirm the presence of nucleotide insertion(s) into vRNAs, the Shimane HA vRNA in purified virions was analyzed by using a deep-sequencing approach. To minimize the background genetic heterogeneity in the virus population, a reassortant virus, rgPR8/Shimane-HA generated from cloned plasmids, was used rather than the parent Shimane strain. The cDNA library was prepared from vRNA without any amplification procedures to minimize the potential errors during the sequencing reaction, and the high depth of coverage of sequencing (approximately 1.8 million reads) enabled to analyze the viral RNA quasispecies, including infrequent nucleotide insertions that might not be detectable in Sanger sequencing. As expected, it was found

that single nucleotide insertions of adenine residues occurred with a comparatively high frequency (65/1812090 of vRNA copies) at nucleotide position 1047 (this is, in fact 1047, 1048, or 1049 since it is not distinguishable which position of these 3 consecutive adenines allowed the adenine insertion) (Fig. 8). Double or triple nucleotide insertions were not detected. These observations indicate that the Shimane vRNA sequence encoding the HA cleavage site naturally has the potential to acquire nontemplate nucleotide insertions and that virus particles carrying the HA segment containing such vRNAs are indeed produced by infected cells. It is also noted that adenines at positions 1047-1049 form a part (junction to the stem) of the loop structure in the predicted secondary structure of the Shimane vRNA (Fig. 9A), suggesting the importance of the loop structure for viral polymerase slippage.

Discussion

In this study, it was demonstrated that the RNA encoding the HA cleavage site of Shimane, originally isolated as a low-pathogenic strain and shown to become highly pathogenic after passaging through experimentally infected chickens, had a potential for acquisition of nontemplate nucleotide insertions. Consecutive adenine residues and enlarged stem-loop structure of the RNA encoding the HA cleavage site of Shimane accelerate the nontemplate nucleotide insertions. And these nucleotide insertions were indeed found in the vRNA incorporating with virus particles.

Secondary structures of RNA molecules are thought to play important roles in the editing mechanism [84]. The editing site of simian virus 5 has a stem-loop structure that is proposed to be essential for the RNA editing activity of the viral polymerase [85]. Similarly, a hairpin-like structure of the ebolavirus GP gene is important for RNA editing [82]. It was recently reported that the nucleotide mutations destabilizing the predicted stem-loop structure just upstream from the editing site of the ebolavirus GP gene dramatically reduced the RNA editing efficiency, whereas other mutations irrelevant to the destabilization of the stem-loop structure did not affect the editing [80]. Thus, we compared the secondary structures of the Linker29, Linker29-24a, and Linker29-24a2b regions and found that all three linker RNAs formed stem-loop structures (Fig. 9). It was noted that Linker29-24a2b had a larger loop than the others, suggesting the possibility that the enlarged stem-loop structure consisting of consecutive adenine and guanine residues accelerated the nucleotide insertion into the RNA sequence encoding the HA cleavage site of Shimane.

Analysis of the predicted secondary structures of RNAs encoding the HA cleavage sites of low pathogenic H5 viruses revealed that most of the RNA encoding the HA cleavage site of low pathogenic H5 viruses formed stem-loop structures containing HA cleavage sites (Fig. 10). For this analysis, all available HA sequences of low pathogenic H5 viruses from the NCBI Influenza Virus Resource Database were used and duplicates were removed. The RNAs encoding the HA cleavage sites of H1 and H3 viruses, not reported previously to become HPAI viruses in natural environment, also formed stem-loop structures, however most of these loops were smaller than the loops formed by the RNAs of H5 viruses and not containing the HA cleavage site (Fig. 11 and 12). And some of the RNAs encoding the HA cleavage sites of H7 viruses, known to have potentials to become HPAI viruses in natural environment, formed stem-loop structures containing the HA cleavage site similar to the stem-loop structures formed by the RNAs of H5 viruses (Fig. 13). Thus these findings suggest that stem-loop structure of the RNAs encoding H5 and H7 viruses might play a key role to acquire the polybasic HA cleavage sites.

Taken together, these data suggest that the RNA editing-like mechanism plays a role in insertion of additional nucleotides into the vRNA region determining the HA cleavage site of Shimane, which might contribute to the creation of the polybasic HA cleavage site. The loop sequence consisting of consecutive adenines/guanines might be favorable to create codons for lysine and/or arginine residues (e.g., AAA, AAG, AGA, and AGG). However, although nucleotide insertion during the viral RNA synthesis was detected, its frequency did not seem to be high enough compared to the RNA editing observed for other viruses [78,81,82]. It is important to note that the HA gene containing only single or double nucleotide insertions into its ORF do not express complete HA molecules due

to frame-shift and that multiples of three nucleotide insertions (i.e., codons such as AAA, AGA) are required to generate a functional HA gene. Further studies are needed to clarify the mechanisms by which HA segments carrying a nonfunctional (i.e., frame-shifted) HA gene can be maintained in the virus population until nucleotide insertions into vRNA of the HA gene are accumulated to create basic amino acid codons during circulation in terrestrial poultry.

Summary

HPAI viruses with the H5 and H7 HA subtypes are known to evolve from low-pathogenic precursors through the acquisition of multiple basic amino acid residues at the HA cleavage site. Although this mechanism is naturally recognized only in the H5 and H7 subtypes, little is known about the genetic basis for the acquisition of the polybasic HA cleavage site. In this study, the reporter assay was established to detect nontemplate nucleotide insertions into the RNA sequence encoding amino acids around the HA cleavage site of a low-pathogenic strain, Shimane, which had been shown to acquire the polybasic HA cleavage site through serial passages in experimentally infected chickens. It was first found that one or two nucleotide insertions into the RNA sequence occurred and that a stretch of adenine residues further enhanced the frequency of the nucleotide insertion. Then it was found that two nucleotide substitutions that had actually occurred prior to the insertion of an arginine residue at the HA cleavage site of Shimane increased the frequency of the nucleotide insertion. Interestingly, the Shimane vRNA corresponding to this sequence was predicted to form a stem-loop structure, and these two nucleotide substitutions enlarged the loop region consisting of consecutive adenine and guanine residues, which likely resulted in increased frequency of nucleotide insertions by viral polymerase slippage. Deep sequencing analyses of the Shimane HA vRNA incorporated into virions revealed that adenine insertions into the particular codons in the loop were indeed observed in approximately 0.0036% of vRNA copies. These data suggest that nucleotide insertions by the RNA editing-like mechanism facilitate the creation of codons for basic amino acids (e.g., AAA, AGA) and might

provide a clue to why the acquisition of the polybasic HA cleavage site is restricted to the particular HA subtypes.

Fig. 5. HA cleavage site sequences of Shimane and its variants passaged in chickens.

Parent Shimane and its variant (24a, 24a2b, and 24a3b) strains obtained during the passage through chickens had different nucleotide and amino acid sequences [21]. Dashes are included to adjust the sequence alignment, and red arrows indicate the HA cleavage sites. The nucleotides and amino acids different from those of the parental Shimane sequence are shown in red.

(A)

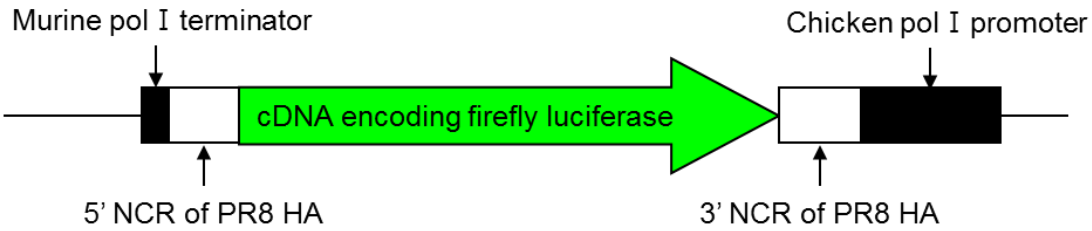

(B)

Linker	Sequence
Linker28	CCCAAAGAGAAACAAGAGGTCTGTTTGG
Linker29	CCCAAAGAGAAACAAGAGGTCTGTTTGGA
Linker29-10A	CCCAAAGAGAAAAAAAAAATCTGTTTGGA
Linker29-24a	CCCAAAGAGAAAAAAGAGGTCTGTTTGGA
Linker29-24a2b	CCCAAAGAAAAAAAAGAGGTCTGTTTGGA
Linker30	CCCAAAGAGAAACAAGAGGTCTGTTTGGAG

(C)

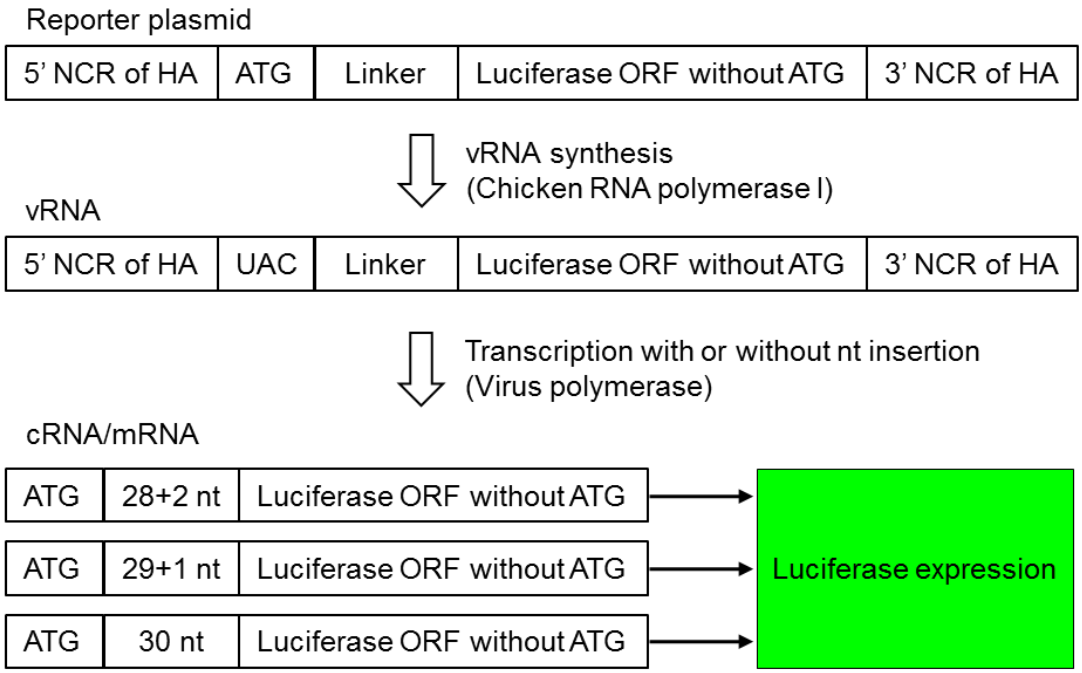

Fig. 6. Reporter assay system to detect nontemplate nucleotide insertions.
The pHW72-LUC-CkpolI plasmid contains firefly luciferase cDNA flanked by the NCRs of the PR8 HA segment, the chicken polI promoter, and the murine polI terminator (A). Nucleotide sequences encoding amino acids around the Shimane HA cleavage site were used as linkers. The nucleotides different from those of the parental

Shimane sequence are indicated in red (B). In this assay, negative sense vRNA was synthesized from transfected pHW72-LUC-CKpolI plasmids, and mRNA and cRNA were transcribed from vRNA with or without nucleotide (nt) insertions.

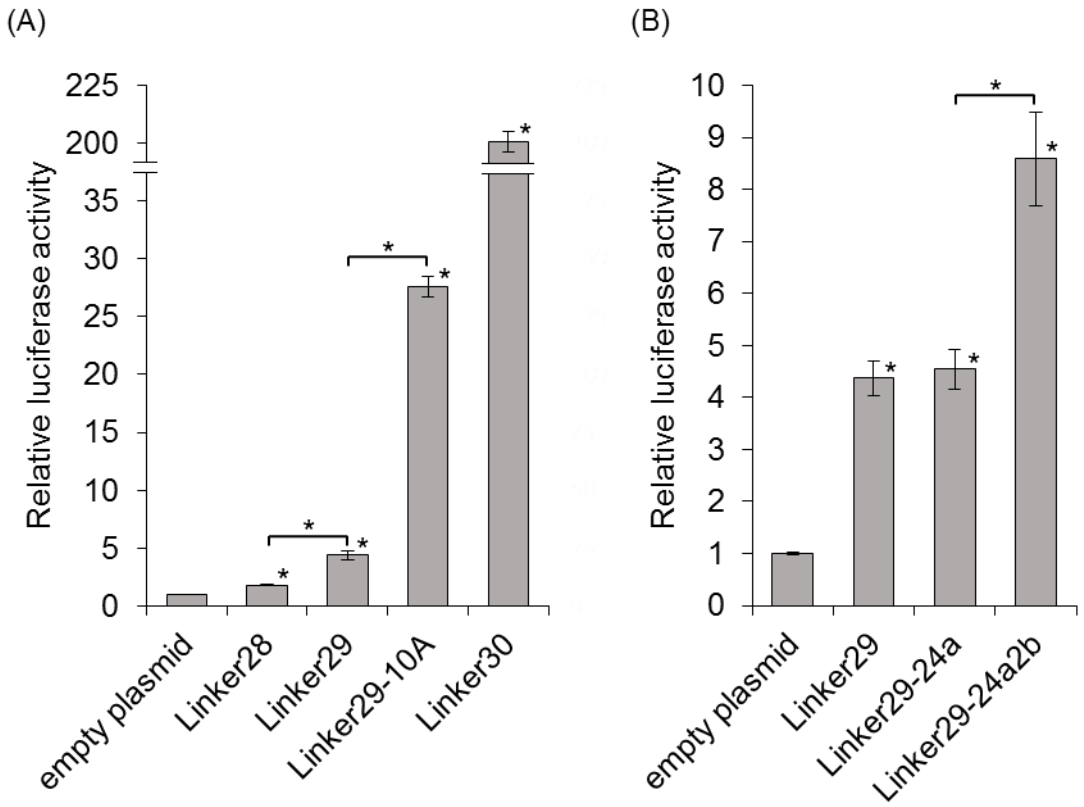

Fig. 7. Luciferase activities in QT6 cells.

QT6 cells were transfected with pHW72-LUC-CKpolI containing the respective linkers, pRL-TK, and a mixture of PB2-, PB1-, PA-, and NP-expressing plasmids. At 24 hours post-transfection, luciferase (firefly and Renilla luciferase) activities were measured. The firefly luciferase activities were standardized using the values given by the transfection control Renilla luciferase activities. Luciferase activities of the empty plasmid, Linker28, Linker29, Linker29-10A, and Linker30 (A) or empty plasmid, Linker29, Linker29-24a, and Linker29-24a2b (B) were compared. Representative data of three independent experiments are shown. Relative luciferase activities are presented as the averages and standard deviations of triplicate wells. Statistical significance was calculated using student's *t*-test (*p<0.01). Asterisks placed directly above the bars indicate significant differences compared to the empty plasmid, and asterisks placed between the bars show significant differences between the indicated bars.

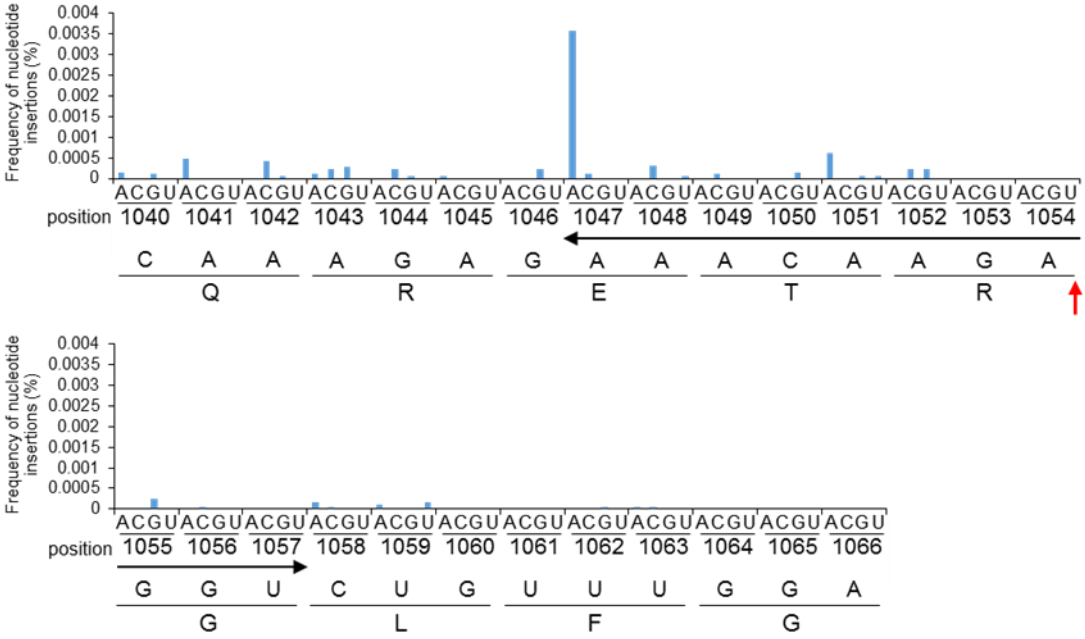

Fig. 8. Deep sequencing analysis of vRNA.

Frequencies of nucleotide insertions into the vRNA encoding the HA cleavage site of Shimane HA are shown. Inserted nucleotide residues, original nucleotides, and amino acid sequences are shown below the horizontal axis. The HA cleavage site is indicated by the red arrow. The black horizontal arrow indicates the sequence (1047-1057) corresponding to the loop structure.

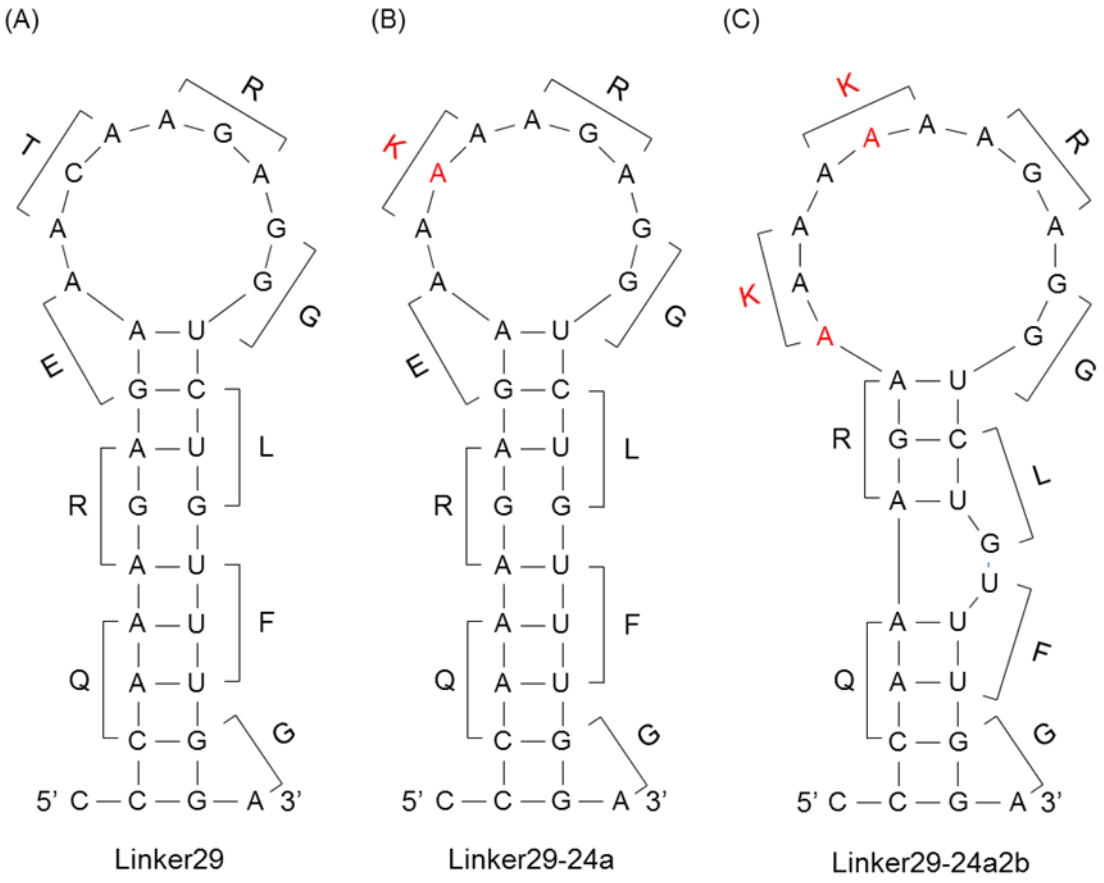

Fig. 9. Secondary RNA structures of the linker regions.

The Mfold RNA secondary structure prediction webserver was used to generate the structures of Linker29 (A), Linker29-24a (B), and Linker29-24a2b (C). Nucleotides and amino acids different from the parental Shimane sequence are shown in red.

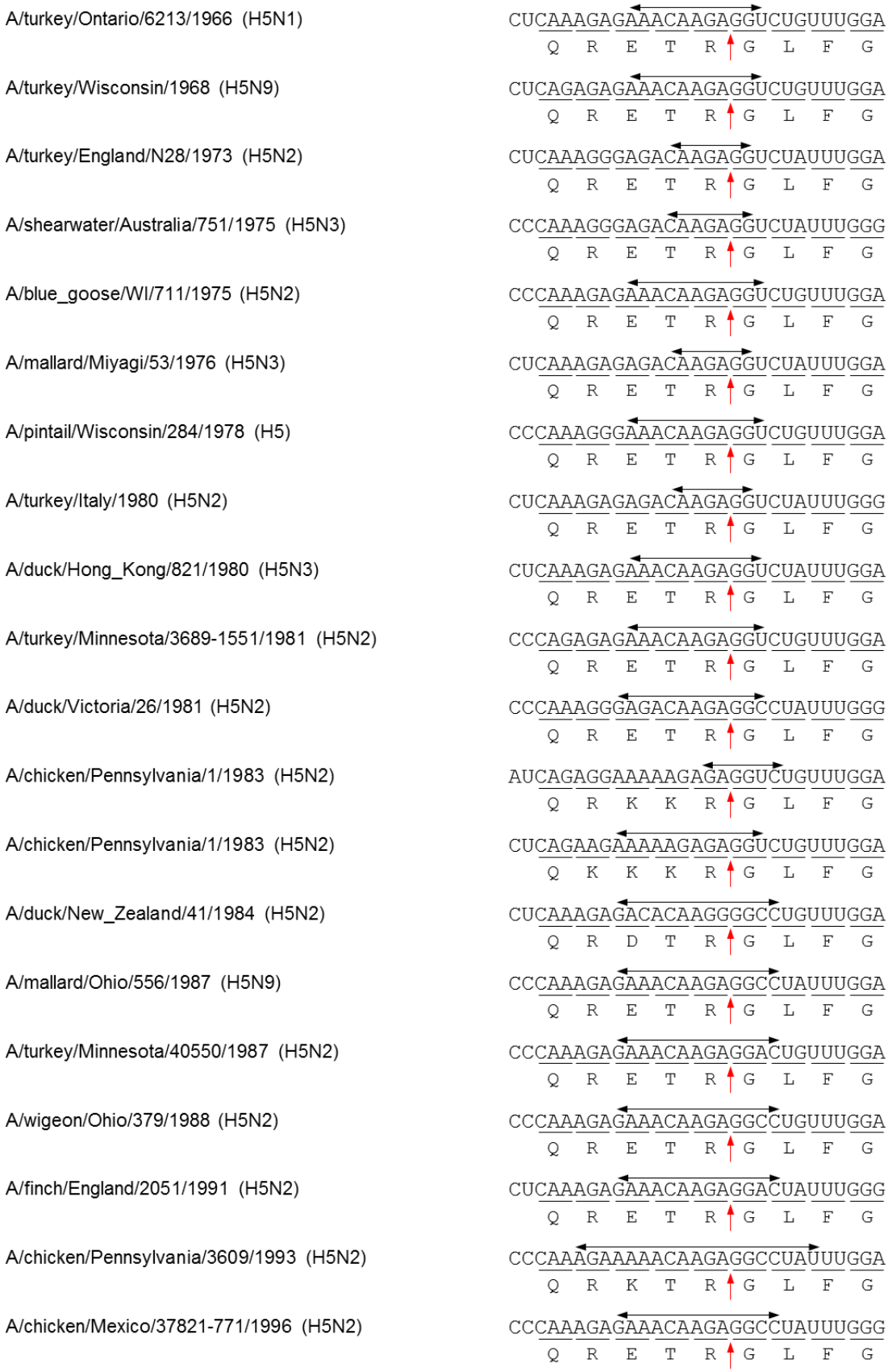
A/turkey/Ontario/6213/1966 (H5N1)
CUCAAAGAGAAACAAGAGGUCUGUUUGGA
Q R E T R G L F G
A/turkey/Wisconsin/1968 (H5N9)
CUCAGAGAGAAACAAGAGGUCUGUUUGGA
Q R E T R G L F G
A/turkey/England/N28/1973 (H5N2)
CUCAAAGGGAGACAAGAGGUCUAUUUGGA
Q R E T R G L F G
A/shearwater/Australia/751/1975 (H5N3)
CCCAAAGGGAGACAAGAGGUCUAUUUGGG
Q R E T R G L F G
A/blue_goose/WI/711/1975 (H5N2)
CCCAAAGAGAAACAAGAGGUCUGUUUGGA
Q R E T R G L F G
A/mallard/Miyagi/53/1976 (H5N3)
CUCAAAGAGAGACAAGAGGUCUAUUUGGA
Q R E T R G L F G
A/pintail/Wisconsin/284/1978 (H5)
CCCAAAGGGAAACAAGAGGUCUGUUUGGA
Q R E T R G L F G
A/turkey/Italy/1980 (H5N2)
CUCAAAGAGAGACAAGAGGUCUAUUUGGG
Q R E T R G L F G
A/duck/Hong_Kong/821/1980 (H5N3)
CUCAAAGAGAAACAAGAGGUCUAUUUGGA
Q R E T R G L F G
A/turkey/Minnesota/3689-1551/1981 (H5N2)
CCCAGAGAGAAACAAGAGGUCUGUUUGGA
Q R E T R G L F G
A/duck/Victoria/26/1981 (H5N2)
CCCAAAGGGAGACAAGAGGCCUAUUUGGG
Q R E T R G L F G
A/chicken/Pennsylvania/1/1983 (H5N2)
AUCAGAGGAAAAAGAGAGGUCUGUUUGGA
Q R K K R G L F G
A/chicken/Pennsylvania/1/1983 (H5N2)
CUCAGAAGAAAAAGAGAGGUCUGUUUGGA
Q K K K R G L F G
A/duck/New_Zealand/41/1984 (H5N2)
CUCAAAGAGACACAAGGGGCCUGUUUGGA
Q R D T R G L F G
A/mallard/Ohio/556/1987 (H5N9)
CCCAAAGAGAAACAAGAGGCCUAUUUGGA
Q R E T R G L F G
A/turkey/Minnesota/40550/1987 (H5N2)
CCCAAAGAGAAACAAGAGGACUGUUUGGA
Q R E T R G L F G
A/wigeon/Ohio/379/1988 (H5N2)
CCCAAAGAGAAACAAGAGGCCUGUUUGGA
Q R E T R G L F G
A/finch/England/2051/1991 (H5N2)
CUCAAAGAGAAACAAGAGGACUAUUUGGG
Q R E T R G L F G
A/chicken/Pennsylvania/3609/1993 (H5N2)
CCCAAAGAAAAACAAGAGGCCUAUUUGGA
Q R K T R G L F G
A/chicken/Mexico/37821-771/1996 (H5N2)
CCCAAAGAGAAACAAGAGGCCUAUUUGGG
Q R E T R G L F G

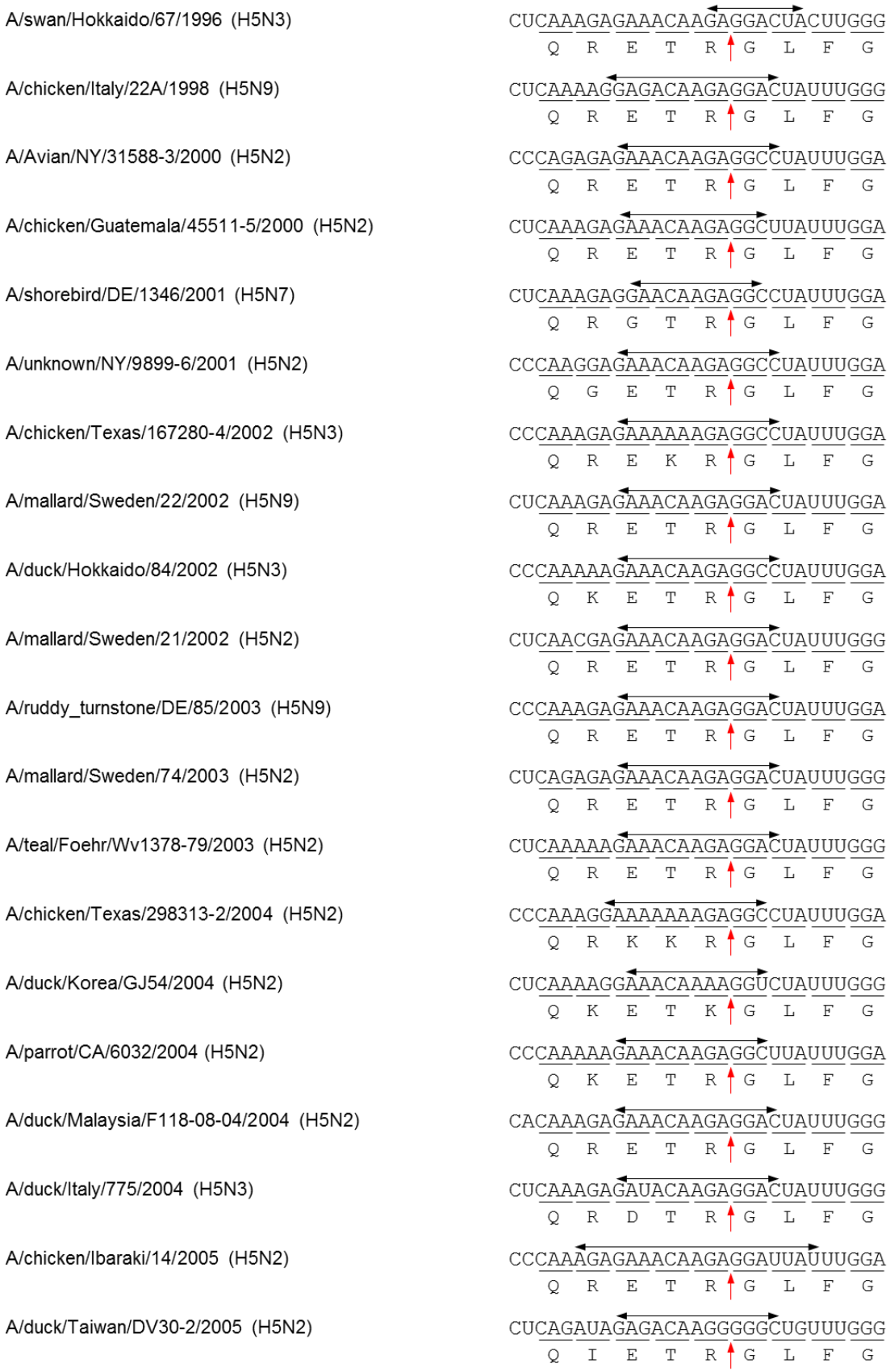
A/swan/Hokkaido/67/1996 (H5N3)
CUCAAAGAGAAACAAGAGGACUACUUGGG
Q R E T R G L F G
A/chicken/Italy/22A/1998 (H5N9)
CUCAAAAGGAGACAAGAGGACUAUUUGGG
Q R E T R G L F G
A/Avian/NY/31588-3/2000 (H5N2)
CCCAGAGAGAAACAAGAGGCCUAUUUGGA
Q R E T R G L F G
A/chicken/Guatemala/45511-5/2000 (H5N2)
CUCAAAGAGAAACAAGAGGCUUAUUUGGA
Q R E T R G L F G
A/shorebird/DE/1346/2001 (H5N7)
CUCAAAGAGGAACAAGAGGCCUAUUUGGA
Q R G T R G L F G
A/unknown/NY/9899-6/2001 (H5N2)
CCCAAGGAGAAACAAGAGGCCUAUUUGGA
Q G E T R G L F G
A/chicken/Texas/167280-4/2002 (H5N3)
CCCAAAGAGAAAAAAGAGGCCUAUUUGGA
Q R E K R G L F G
A/mallard/Sweden/22/2002 (H5N9)
CUCAAAGAGAAACAAGAGGACUAUUUGGA
Q R E T R G L F G
A/duck/Hokkaido/84/2002 (H5N3)
CCCAAAAAGAAACAAGAGGCCUAUUUGGA
Q K E T R G L F G
A/mallard/Sweden/21/2002 (H5N2)
CUCAACGAGAAACAAGAGGACUAUUUGGG
Q R E T R G L F G
A/ruddy_turnstone/DE/85/2003 (H5N9)
CCCAAAGAGAAACAAGAGGACUAUUUGGA
Q R E T R G L F G
A/mallard/Sweden/74/2003 (H5N2)
CUCAGAGAGAAACAAGAGGACUAUUUGGG
Q R E T R G L F G
A/teal/Foehr/Wv1378-79/2003 (H5N2)
CUCAAAAAGAAACAAGAGGACUAUUUGGG
Q R E T R G L F G
A/chicken/Texas/298313-2/2004 (H5N2)
CCCAAAGGAAAAAAAGAGGCCUAUUUGGA
Q R K K R G L F G
A/duck/Korea/GJ54/2004 (H5N2)
CUCAAAAGGAAACAAAAGGUCUAUUUGGG
Q K E T K G L F G
A/parrot/CA/6032/2004 (H5N2)
CCCAAAAAGAAACAAGAGGCUUAUUUGGA
Q K E T R G L F G
A/duck/Malaysia/F118-08-04/2004 (H5N2)
CACAAAGAGAAACAAGAGGACUAUUUGGG
Q R E T R G L F G
A/duck/Italy/775/2004 (H5N3)
CUCAAAGAGAUACAAGAGGACUAUUUGGG
Q R D T R G L F G
A/chicken/Ibaraki/14/2005 (H5N2)
CCCAAAGAGAAACAAGAGGAUUAUUUGGA
Q R E T R G L F G
A/duck/Taiwan/DV30-2/2005 (H5N2)
CUCAGAUAGAGACAAGGGGGCUGUUUGGG
Q I E T R G L F G

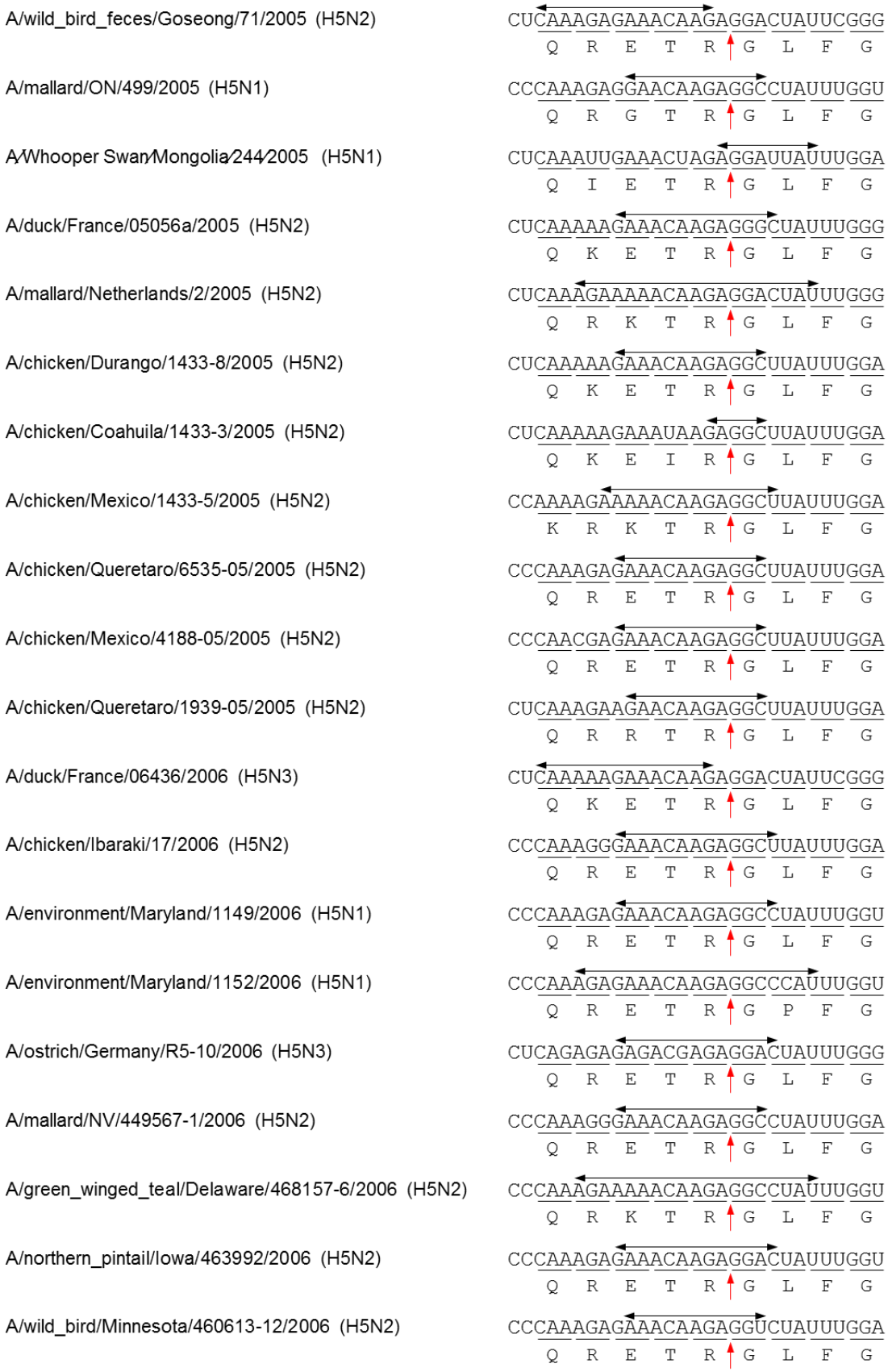
A/wild_bird_feces/Goseong/71/2005 (H5N2)
CUCAAAGAGAAACAAGAGGACUAUUCGGG
Q R E T R G L F G
A/mallard/ON/499/2005 (H5N1)
CCCAAAGAGGAACAAGAGGCCUAUUUGGU
Q R G T R G L F G
A/Whooper Swan/Mongolia/244/2005 (H5N1)
CUCAAAUUGAAACUAGAGGAUUAUUUGGA
Q I E T R G L F G
A/duck/France/05056a/2005 (H5N2)
CUCAAAAAGAAACAAGAGGGCUAUUUGGG
Q K E T R G L F G
A/mallard/Netherlands/2/2005 (H5N2)
CUCAAAGAAAAACAAGAGGACUAUUUGGG
Q R K T R G L F G
A/chicken/Durango/1433-8/2005 (H5N2)
CUCAAAAAGAAACAAGAGGCUUAUUUGGA
Q K E T R G L F G
A/chicken/Coahuila/1433-3/2005 (H5N2)
CUCAAAAAGAAAUAAGAGGCUUAUUUGGA
Q K E I R G L F G
A/chicken/Mexico/1433-5/2005 (H5N2)
CCAAAAGAAAAACAAGAGGCUUAUUUGGA
K R K T R G L F G
A/chicken/Queretaro/6535-05/2005 (H5N2)
CCCAAAGAGAAACAAGAGGCUUAUUUGGA
Q R E T R G L F G
A/chicken/Mexico/4188-05/2005 (H5N2)
CCCAACGAGAAACAAGAGGCUUAUUUGGA
Q R E T R G L F G
A/chicken/Queretaro/1939-05/2005 (H5N2)
CUCAAAGAAGAACAAGAGGCUUAUUUGGA
Q R R T R G L F G
A/duck/France/06436/2006 (H5N3)
CUCAAAAAGAAACAAGAGGACUAUUCGGG
Q K E T R G L F G
A/chicken/Ibaraki/17/2006 (H5N2)
CCCAAAGGGAAACAAGAGGCUUAUUUGGA
Q R E T R G L F G
A/environment/Maryland/1149/2006 (H5N1)
CCCAAAGAGAAACAAGAGGCCUAUUUGGU
Q R E T R G L F G
A/environment/Maryland/1152/2006 (H5N1)
CCCAAAGAGAAACAAGAGGCCCAUUUGGU
Q R E T R G P F G
A/ostrich/Germany/R5-10/2006 (H5N3)
CUCAGAGAGAGACGAGAGGACUAUUUGGG
Q R E T R G L F G
A/mallard/NV/449567-1/2006 (H5N2)
CCCAAAGGGAAACAAGAGGCCUAUUUGGA
Q R E T R G L F G
A/green_winged_teal/Delaware/468157-6/2006 (H5N2)
CCCAAAGAAAAACAAGAGGCCUAUUUGGU
Q R K T R G L F G
A/northern_pintail/Iowa/463992/2006 (H5N2)
CCCAAAGAGAAACAAGAGGACUAUUUGGU
Q R E T R G L F G
A/wild_bird/Minnesota/460613-12/2006 (H5N2)
CCCAAAGAGAAACAAGAGGUCUAUUUGGA
Q R E T R G L F G

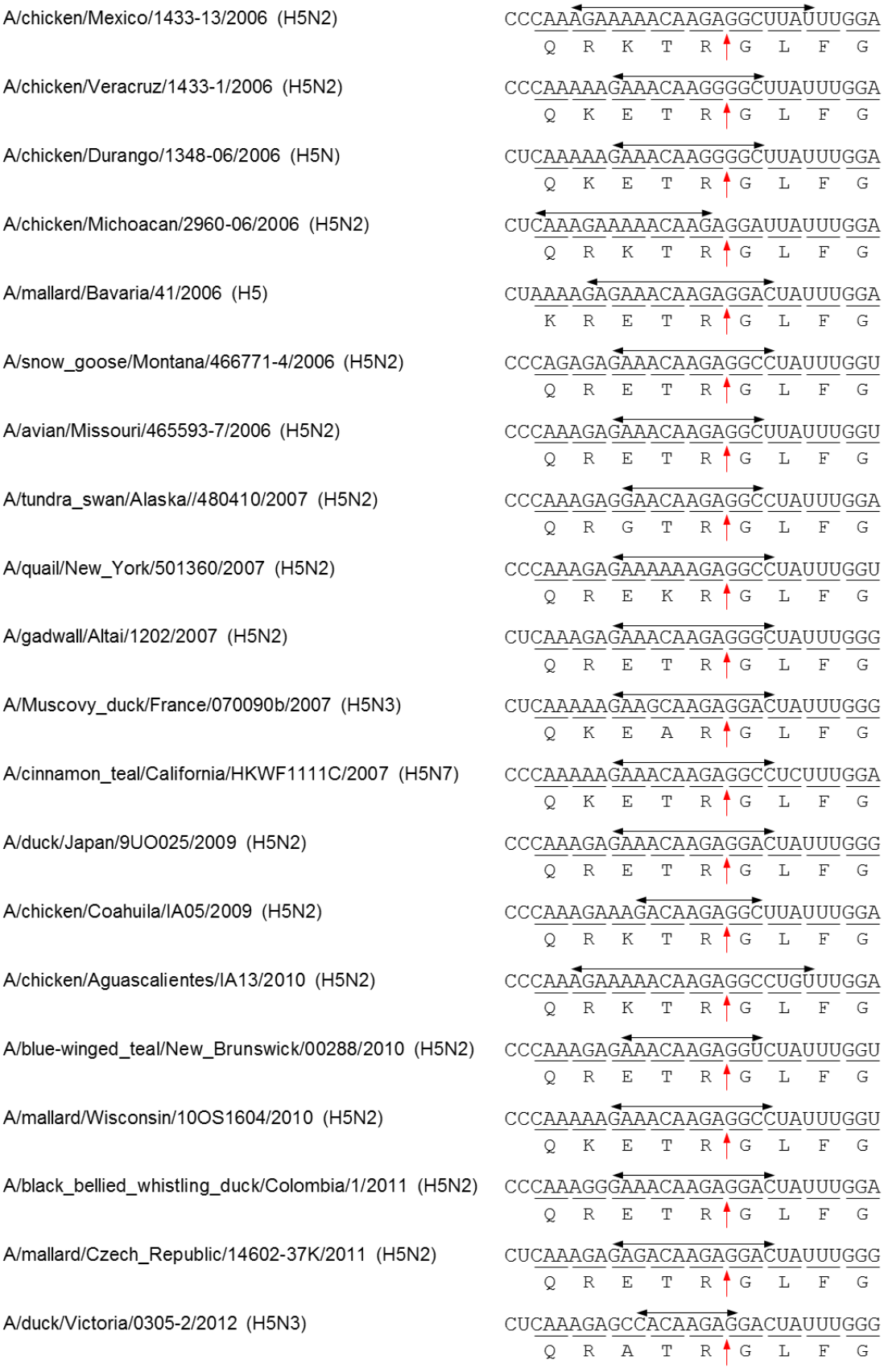
A/chicken/Mexico/1433-13/2006 (H5N2)
CCCAAAGAAAAACAAGAGGCUUAUUUGGA
Q R K T R G L F G
A/chicken/Veracruz/1433-1/2006 (H5N2)
CCCAAAAAGAAACAAGGGGCUUAUUUGGA
Q K E T R G L F G
A/chicken/Durango/1348-06/2006 (H5N)
CUCAAAAAGAAACAAGGGGCUUAUUUGGA
Q K E T R G L F G
A/chicken/Michoacan/2960-06/2006 (H5N2)
CUCAAAGAAAAACAAGAGGAUUAUUUGGA
Q R K T R G L F G
A/mallard/Bavaria/41/2006 (H5)
CUAAAAGAGAAACAAGAGGACUAUUUGGA
K R E T R G L F G
A/snow_goose/Montana/466771-4/2006 (H5N2)
CCCAGAGAGAAACAAGAGGCCUAUUUGGU
Q R E T R G L F G
A/avian/Missouri/465593-7/2006 (H5N2)
CCCAAAGAGAAACAAGAGGCUUAUUUGGU
Q R E T R G L F G
A/tundra_swan/Alaska//480410/2007 (H5N2)
CCCAAAGAGGAACAAGAGGCCUAUUUGGA
Q R G T R G L F G
A/quail/New_York/501360/2007 (H5N2)
CCCAAAGAGAAAAAAGAGGCCUAUUUGGU
Q R E K R G L F G
A/gadwall/Altai/1202/2007 (H5N2)
CUCAAAGAGAAACAAGAGGGCUAUUUGGG
Q R E T R G L F G
A/Muscovy_duck/France/070090b/2007 (H5N3)
CUCAAAAAGAAGCAAGAGGACUAUUUGGG
Q K E A R G L F G
A/cinnamon_teal/California/HKWF1111C/2007 (H5N7)
CCCAAAAAGAAACAAGAGGCCUCUUUGGA
Q K E T R G L F G
A/duck/Japan/9UO025/2009 (H5N2)
CCCAAAGAGAAACAAGAGGACUAUUUGGG
Q R E T R G L F G
A/chicken/Coahuila/IA05/2009 (H5N2)
CCCAAAGAAAGACAAGAGGCUUAUUUGGA
Q R K T R G L F G
A/chicken/Aguascalientes/IA13/2010 (H5N2)
CCCAAAGAAAAACAAGAGGCCUGUUUGGA
Q R K T R G L F G
A/blue-winged_teal/New_Brunswick/00288/2010 (H5N2)
CCCAAAGAGAAACAAGAGGUCUAUUUGGU
Q R E T R G L F G
A/mallard/Wisconsin/10OS1604/2010 (H5N2)
CCCAAAAAGAAACAAGAGGCCUAUUUGGU
Q K E T R G L F G
A/black_bellied_whistling_duck/Colombia/1/2011 (H5N2)
CCCAAAGGGAAACAAGAGGACUAUUUGGA
Q R E T R G L F G
A/mallard/Czech_Republic/14602-37K/2011 (H5N2)
CUCAAAGAGAGACAAGAGGACUAUUUGGG
Q R E T R G L F G
A/duck/Victoria/0305-2/2012 (H5N3)
CUCAAAGAGCCACAAGAGGACUAUUUGGG
Q R A T R G L F G

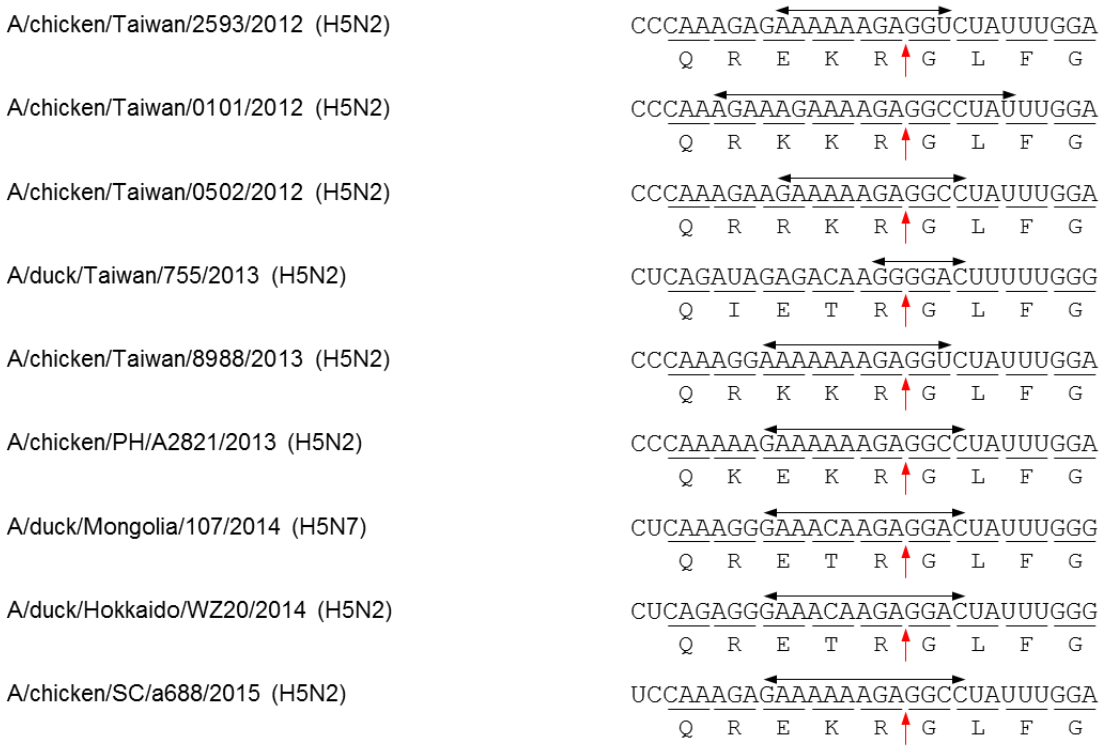

Fig. 10. Sequences and secondary structures of the RNAs encoding the HA cleavage sites of low pathogenic H5 viruses.

All available RNA sequences of the HA cleavage site of low pathogenic H5 viruses are shown. Data were obtained from the NCBI Influenza Virus Resource Database and duplicates were removed. Amino acid sequences are shown below the RNA sequences and the HA cleavage sites are indicated by the red arrows. The black horizontal arrows indicate the sequences corresponding to the loop structures.

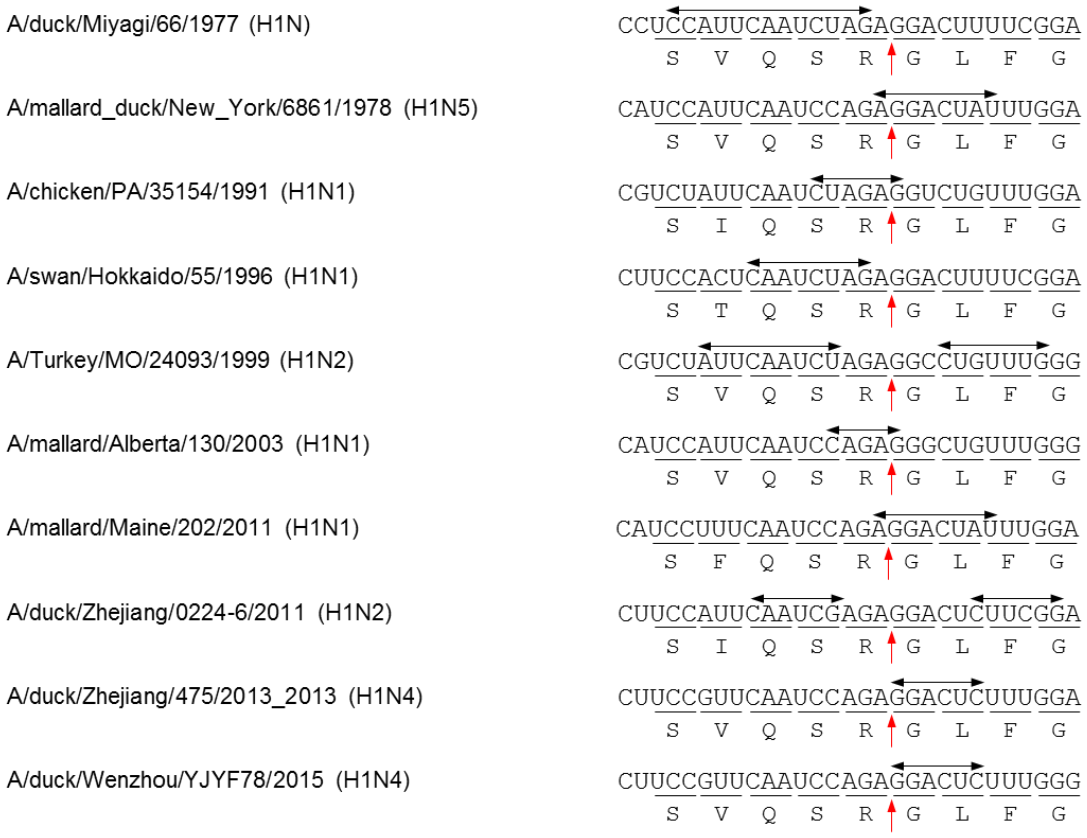

Fig. 11. Sequences and secondary structures of the RNAs encoding the HA cleavage sites of H1 viruses.

Representative RNA sequences of the HA cleavage site of H1 viruses are shown. Data were obtained from the NCBI Influenza Virus Resource Database. Amino acid sequences are shown below the RNA sequences and the HA cleavage sites are indicated by the red arrows. The black horizontal arrows indicate the sequences corresponding to the loop structures.

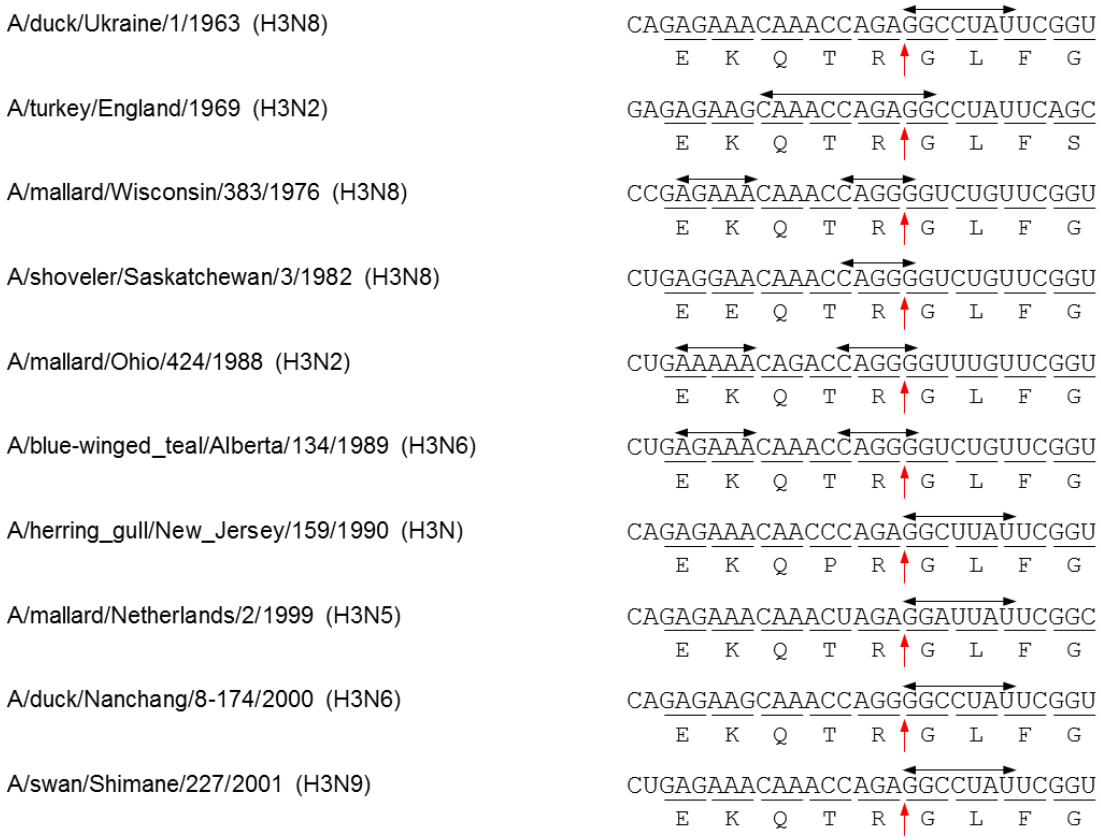

Fig. 12. Sequences and secondary structures of the RNAs encoding the HA cleavage sites of H3 viruses.

Representative RNA sequences of the HA cleavage site of H3 viruses are shown. Data were obtained from the NCBI Influenza Virus Resource Database. Amino acid sequences are shown below the RNA sequences and the HA cleavage sites are indicated by the red arrows. The black horizontal arrows indicate the sequences corresponding to the loop structures.

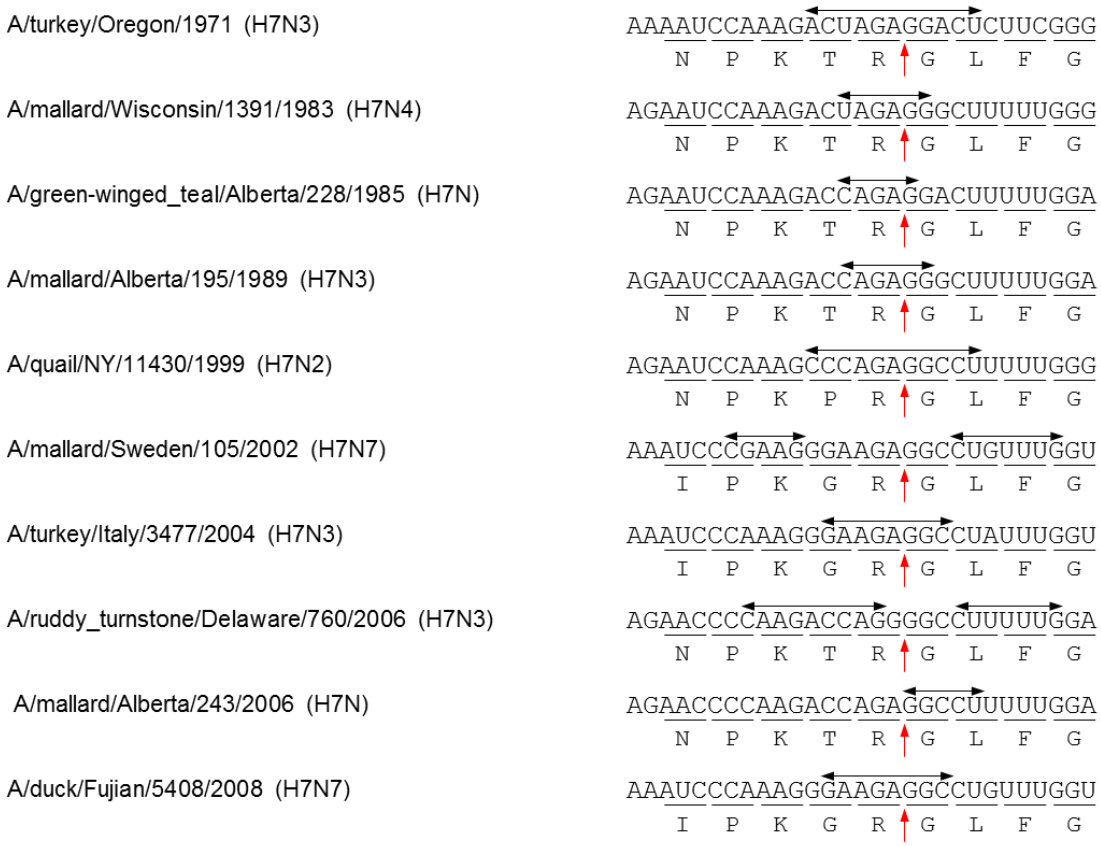

Fig. 13. Sequences and secondary structures of the RNAs encoding the HA cleavage sites of low pathogenic H7 viruses.

Representative RNA sequences of the HA cleavage site of low pathogenic H7 viruses are shown. Data were obtained from the NCBI Influenza Virus Resource Database and duplicates were removed. Amino acid sequences are shown below the RNA sequences and the HA cleavage sites are indicated by the red arrows. The black horizontal arrows indicate the sequences corresponding to the loop structures.

Conclusion

HPAI viruses cause an extremely infectious, systemic disease characterized by necrobiotic, hemorrhagic, or inflammatory lesions in multiple organs in poultry, and are sporadically transmitted to humans, resulting in severe and potentially fatal pneumonia. Despite extensive control efforts, HPAI viruses continue to circulate worldwide and pose serious threats to both human and animal health. The present study provides information on the genetic basis and mechanisms underlying the pathogenicity of H5N1 HPAI viruses.

In chapter I, the author compared the pathogenicity of two H5N1 HPAI viruses, WZ83 and WZ101, which are almost genetically identical but differ in pathogenicity for chickens. It was found that the amino acid at position 43 in the M1 protein was responsible for the higher pathogenicity of WZ101 than WZ83 in chickens, ducks, and mice. This amino acid also affected the *in vitro* replication capacity of WZ83 and WZ101 and the stability of the viral M1 protein in infected cells. Although the underlying mechanisms remain to be determined, these results indicate that the amino acid at position 43 of the M1 protein can be a critical factor contributing to the high pathogenicity of H5N1 HPAI viruses in both avian and mammalian species.

In chapter II, using an H5N3 low pathogenic avian influenza virus, which was shown to evolve to a HPAI virus by acquiring basic amino acid residues at the HA cleavage site through serial passage in experimentally infected chickens, the author investigated a genetic basis for the acquisition of the polybasic HA cleavage site. It was found that consecutive adenine residues and an enlarged stem-loop structure of vRNA accelerated nontemplate nucleotide insertions into the vRNA sequence encoding the HA cleavage site and that such insertions were indeed found in the vRNA incorporating into

virus particles. These results suggest that the vRNA secondary structure plays a key role in inducing viral polymerase slippage, resulting in increased frequency of nucleotide (adenine and guanine) insertions, which may contribute to the creation of the polybasic HA cleavage site. These findings may provide a clue to why the acquisition of the polybasic HA cleavage site is restricted to particular HA subtypes.

In this thesis, the author demonstrated a novel molecular determinant of virulence of H5N1 HPAI viruses for both mammalian and avian species and a genetic basis for the acquisition of basic amino acid residues at the H5 HA cleavage site. The findings of the present study underscore the importance of continuous global monitoring of avian influenza viruses to better understand their ecology in nature and also to take preemptive measures to minimize the risk of transmission to domestic animals and humans.

Acknowledgement

I would like to particularly acknowledgement to Professor Ayato Takada (Division of Global Epidemiology, Hokkaido University Research Center for Zoonosis Control, Sapporo, Japan), for his valuable advice, suggestions, and support for my course as well as many leaning opportunities and experiences.

I sincerely appreciate the valuable suggestions and advice from Professor Hirofumi Sawa (Division of Molecular Pathology, Hokkaido University Research Center for Zoonosis Control, Sapporo, Japan), Professor Yoshihiro Sakoda (Laboratory of Microbiology, Department of Disease Control, Graduate School of Veterinary Medicine, Hokkaido University, Sapporo, Japan), and Professor Kazuhiko Ohashi (Laboratory of Infectious Disease, Department of Disease Control, Graduate School of Veterinary Medicine, Hokkaido University, Sapporo, Japan).

I would like to specially thank Associate Professor Manabu Igarashi, Assistant Professor Reiko Yoshida, Assistant Professor Rashid Manzoor, and Ms. Hiroko Miyamoto (Division of Global Epidemiology, Hokkaido University Research Center for Zoonosis Control, Sapporo, Japan) for their technical and academic support and advice. I would also like to thank to all the members of the Division of Global Epidemiology for their kind and heartfelt support during my course.

I would like to thank Professor Takashi Kimura (Laboratory of Comparative Pathology, Department of Veterinary Clinical Sciences, Graduate School of Veterinary

Medicine, Hokkaido University, Sapporo, Japan) for kindly teaching me excellent pathological techniques. I would also like to thank Ms. Aiko Ohnuma (Administration Office, Research Center for Zoonosis Control, Hokkaido University, Sapporo, Japan) for her excellent technical support. And I really thank Assistant Professor Michael Henshaw (English as a Foreign Language, Graduate School of Veterinary Medicine, Hokkaido University, Sapporo, Japan) for his excellent and interesting English lectures.

I am really thankful to Professor Tsukasa Seya (Department of Microbiology and Immunology, Graduate School of Medicine, Hokkaido University, Sapporo Japan) for providing me with the opportunity to study virology in this laboratory.

I am extremely grateful to Dr. Akira Suzuki, Dr. Sari Iwasaki (Diagnostic Pathology, KKR Sapporo Medical Center, Sapporo, Japan) and the members of Diagnostic Pathology (KKR Sapporo Medical Center, Sapporo, Japan) for their kind instruction in clinical pathology and deep understanding of my research.

I wish to thank all the members of the Hokkaido University Research Center for Zoonosis Control (Sapporo, Japan) and Graduate School of Veterinary Medicine (Hokkaido University, Sapporo, Japan) for their help, encouragement, and kindness.

Special thanks to my parents for their heartfelt and unlimited support throughout my life. Finally, I would like to express deepest gratitude to my wife Yurina for her continuous support and encouragement of my work.

References

1. Webster RG, Bean WJ, Gorman OT, Chambers TM, Kawaoka Y (1992) Evolution and ecology of influenza A viruses. Microbiol Rev 56: 152-179.
2. Tong S, Li Y, Rivailler P, Conrardy C, Castillo DA, Chen LM, Recuenco S, Ellison JA, Davis CT, York IA, Turmelle AS, Moran D, Rogers S, Shi M, Tao Y, Weil MR, Tang K, Rowe LA, Sammons S, Xu X, Frace M, Lindblade KA, Cox NJ, Anderson LJ, Rupprecht CE, Donis RO (2012) A distinct lineage of influenza A virus from bats. Proc Natl Acad Sci USA 109: 4269-4274.
3. Tong S, Zhu X, Li Y, Shi M, Zhang J, Bourgeois M, Yang H, Chen X, Recuenco S, Gomez J, Chen LM, Johnson A, Tao Y, Dreyfus C, Yu W, McBride R, Carney PJ, Gilbert AT, Chang J, Guo Z, Davis CT, Paulson JC, Stevens J, Rupprecht CE, Holmes EC, Wilson IA, Donis RO (2013) New world bats harbor diverse influenza A viruses. PLoS Pathog 9: e1003657.
4. Ito T, Okazaki K, Kawaoka Y, Takada A, Webster RG, Kida H (1995) Perpetuation of influenza A viruses in Alaskan waterfowl reservoirs. Arch Virol 140: 1163-1172.
5. Okazaki K, Takada A, Ito T, Imai M, Takakuwa H, Hatta M, Ozaki H, Tanizaki T, Nagano T, Ninomiya A, Demenev VA, Tyaptirganov MM, Karatayeva TD, Yamnikova SS, Lvov DK, Kida H (2000) Precursor genes of future pandemic influenza viruses are perpetuated in ducks nesting in Siberia. Arch Virol 145: 885-893.
6. Alexander DJ (2000) A review of avian influenza in different bird species. Vet Microbiol 74: 3-13.
7. Swayne DE, Suarez DL (2000) Highly pathogenic avian influenza. Rev Sci Tech 19: 463-482.

8. Smith GJ, Fan XH, Wang J, Li KS, Qin K, Zhang JX, Vijaykrishna D, Cheung CL, Huang K, Rayner JM, Peiris JS, Chen H, Webster RG, Guan Y (2006) Emergence and predominance of an H5N1 influenza variant in China. Proc Natl Acad Sci U S A 103: 16936-16941.
9. Control CfD, Prevention (1997) Isolation of avian influenza A (H5N1) viruses from humans--Hong Kong, May-December 1997. MMWR Morb Mortal Wkly Rep 46: 1204.
10. Shortridge KF, Zhou NN, Guan Y, Gao P, Ito T, Kawaoka Y, Kodihalli S, Krauss S, Markwell D, Murti KG, Norwood M, Senne D, Sims L, Takada A, Webster RG (1998) Characterization of avian H5N1 influenza viruses from poultry in Hong Kong. Virology 252: 331-342.
11. Webster RG, Peiris M, Chen H, Guan Y (2006) H5N1 outbreaks and enzootic influenza. Emerg Infect Dis 12: 3-8.
12. Sturm-Ramirez KM, Ellis T, Bousfield B, Bissett L, Dyrting K, Rehg JE, Poon L, Guan Y, Peiris M, Webster RG (2004) Reemerging H5N1 influenza viruses in Hong Kong in 2002 are highly pathogenic to ducks. J Virol 78: 4892-4901.
13. Chen H, Smith GJ, Zhang SY, Qin K, Wang J, Li KS, Webster RG, Peiris JS, Guan Y (2005) Avian flu: H5N1 virus outbreak in migratory waterfowl. Nature 436: 191-192.
14. Kerkhove MD (2013) Brief literature review for the WHO global influenza research agenda–highly pathogenic avian influenza H5N1 risk in humans. Influenza Other Respir Viruses 7: 26-33.
15. Banks J, Speidel ES, Moore E, Plowright L, Piccirillo A, Capua I, Cordioli P, Fioretti A, Alexander DJ (2001) Changes in the haemagglutinin and the neuraminidase genes prior to the emergence of highly pathogenic H7N1 avian influenza viruses in Italy.

Arch Virol 146: 963-973.

16. Horimoto T, Kawaoka Y (1994) Reverse genetics provides direct evidence for a correlation of hemagglutinin cleavability and virulence of an avian influenza A virus. J Virol 68: 3120-3128.

17. Horimoto T, Rivera E, Pearson J, Senne D, Krauss S, Kawaoka Y, Webster RG (1995) Origin and molecular changes associated with emergence of a highly pathogenic H5N2 influenza virus in Mexico. Virology 213: 223-230.

18. Kawaoka Y, Naeve CW, Webster RG (1984) Is virulence of H5N2 influenza viruses in chickens associated with loss of carbohydrate from the hemagglutinin? Virology 139: 303-316.

19. Senne DA, Panigrahy B, Kawaoka Y, Pearson JE, Suss J, Lipkind M, Kida H, Webster RG (1996) Survey of the hemagglutinin (HA) cleavage site sequence of H5 and H7 avian influenza viruses: amino acid sequence at the HA cleavage site as a marker of pathogenicity potential. Avian Dis 40: 425-437.

20. Garcia M, Crawford JM, Latimer JW, Rivera-Cruz E, Perdue ML (1996) Heterogeneity in the haemagglutinin gene and emergence of the highly pathogenic phenotype among recent H5N2 avian influenza viruses from Mexico. J Gen Virol 77: 1493-1504.

21. Ito T, Goto H, Yamamoto E, Tanaka H, Takeuchi M, Kuwayama M, Kawaoka Y, Otsuki K (2001) Generation of a highly pathogenic avian influenza A virus from an avirulent field isolate by passaging in chickens. J Virol 75: 4439-4443.

22. Spackman E, Senne DA, Davison S, Suarez DL (2003) Sequence analysis of recent H7 avian influenza viruses associated with three different outbreaks in commercial poultry in the United States. J Virol 77: 13399-13402.

23. Suarez DL, Senne DA, Banks J, Brown IH, Essen SC, Lee CW, Manvell RJ, Mathieu-Benson C, Moreno V, Pedersen JC, Panigrahy B, Rojas H, Spackman E, Alexander DJ (2004) Recombination resulting in virulence shift in avian influenza outbreak, Chile. Emerg Infect Dis 10: 693-699.

24. Pasick J, Handel K, Robinson J, Copps J, Ridd D, Hills K, Kehler H, Cottam-Birt C, Neufeld J, Berhane Y, Czub S (2005) Intersegmental recombination between the haemagglutinin and matrix genes was responsible for the emergence of a highly pathogenic H7N3 avian influenza virus in British Columbia. J Gen Virol 86: 727-731.

25. Maurer-Stroh S, Lee RT, Gunalan V, Eisenhaber F (2013) The highly pathogenic H7N3 avian influenza strain from July 2012 in Mexico acquired an extended cleavage site through recombination with host 28S rRNA. Virol J 10: 139.

26. Gohrbandt S, Veits J, Hundt J, Bogs J, Breithaupt A, Teifke JP, Weber S, Mettenleiter TC, Stech J (2011) Amino acids adjacent to the haemagglutinin cleavage site are relevant for virulence of avian influenza viruses of subtype H5. J Gen Virol 92: 51-59.

27. Hatta M, Gao P, Halfmann P, Kawaoka Y (2001) Molecular basis for high virulence of Hong Kong H5N1 influenza A viruses. Science 293: 1840-1842.

28. Li Z, Chen H, Jiao P, Deng G, Tian G, Li Y, Hoffmann E, Webster RG, Matsuoka Y, Yu K (2005) Molecular basis of replication of duck H5N1 influenza viruses in a mammalian mouse model. J Virol 79: 12058-12064.

29. Salomon R, Franks J, Govorkova EA, Ilyushina NA, Yen HL, Hulse-Post DJ, Humberd J, Trichet M, Rehg JE, Webby RJ, Webster RG, Hoffmann E (2006) The polymerase complex genes contribute to the high virulence of the human H5N1

influenza virus isolate A/Vietnam/1203/04. J Exp Med 203: 689-697.

30. Song J, Feng H, Xu J, Zhao D, Shi J, Li Y, Deng G, Jiang Y, Li X, Zhu P, Guan Y, Bu Z, Kawaoka Y, Chen H (2011) The PA protein directly contributes to the virulence of H5N1 avian influenza viruses in domestic ducks. J Virol 85: 2180-2188.

31. Matrosovich M, Zhou N, Kawaoka Y, Webster R (1999) The surface glycoproteins of H5 influenza viruses isolated from humans, chickens, and wild aquatic birds have distinguishable properties. J Virol 73: 1146-1155.

32. Li KS, Guan Y, Wang J, Smith GJ, Xu KM, Duan L, Rahardjo AP, Puthavathana P, Buranathai C, Nguyen TD, Estoepangestie AT, Chaisingh A, Auewarakul P, Long HT, Hanh NT, Webby RJ, Poon LL, Chen H, Shortridge KF, Yuen KY, Webster RG, Peiris JS (2004) Genesis of a highly pathogenic and potentially pandemic H5N1 influenza virus in eastern Asia. Nature 430: 209-213.

33. Talon J, Salvatore M, O'Neill RE, Nakaya Y, Zheng H, Muster T, Garcia-Sastre A, Palese P (2000) Influenza A and B viruses expressing altered NS1 proteins: A vaccine approach. Proc Natl Acad Sci USA 97: 4309-4314.

34. Seo SH, Hoffmann E, Webster RG (2002) Lethal H5N1 influenza viruses escape host anti-viral cytokine responses. Nat Med 8: 950-954.

35. Jiao P, Tian G, Li Y, Deng G, Jiang Y, Liu C, Liu W, Bu Z, Kawaoka Y, Chen H (2008) A single-amino-acid substitution in the NS1 protein changes the pathogenicity of H5N1 avian influenza viruses in mice. J Virol 82: 1146-1154.

36. Zaraket H, Bridges OA, Russell CJ (2013) The pH of activation of the hemagglutinin protein regulates H5N1 influenza virus replication and pathogenesis in mice. J Virol 87: 4826-4834.

37. Tan L, Su S, Smith DK, He S, Zheng Y, Shao Z, Ma J, Zhu H, Zhang G (2014) A

combination of HA and PA mutations enhances virulence in a mouse-adapted H6N6 influenza A virus. J Virol 88: 14116-14125.

38. Fan S, Deng G, Song J, Tian G, Suo Y, Jiang Y, Guan Y, Bu Z, Kawaoka Y, Chen H (2009) Two amino acid residues in the matrix protein M1 contribute to the virulence difference of H5N1 avian influenza viruses in mice. Virology 384: 28-32.

39. Kajihara M, Sakoda Y, Soda K, Minari K, Okamatsu M, Takada A, Kida H (2013) The PB2, PA, HA, NP, and NS genes of a highly pathogenic avian influenza virus A/whooper swan/Mongolia/3/2005 (H5N1) are responsible for pathogenicity in ducks. Virol J 10: 45.

40. Hatta M, Neumann G, Kawaoka Y (2001) Reverse genetics approach towards understanding pathogenesis of H5N1 Hong Kong influenza A virus infection. Philos Trans R Soc Lond B Biol Sci 356: 1841-1843.

41. Kishida N, Sakoda Y, Isoda N, Matsuda K, Eto M, Sunaga Y, Umemura T, Kida H (2005) Pathogenicity of H5 influenza viruses for ducks. Arch Virol 150: 1383-1392.

42. Sakoda Y, Sugar S, Batchluun D, Erdene-Ochir TO, Okamatsu M, Isoda N, Soda K, Takakuwa H, Tsuda Y, Yamamoto N, Kishida N, Matsuno K, Nakayama E, Kajihara M, Yokoyama A, Takada A, Sodnomdarjaa R, Kida H (2010) Characterization of H5N1 highly pathogenic avian influenza virus strains isolated from migratory waterfowl in Mongolia on the way back from the southern Asia to their northern territory. Virology 406: 88-94.

43. Kajihara M, Matsuno K, Simulundu E, Muramatsu M, Noyori O, Manzoor R, Nakayama E, Igarashi M, Tomabechi D, Yoshida R, Okamatsu M, Sakoda Y, Ito K, Kida H, Takada A (2011) An H5N1 highly pathogenic avian influenza virus that invaded Japan through waterfowl migration. Jpn J Vet Res 59: 89-100.

44. Zimmermann T, Schaefer W (1960) Effect of p-fluorophenyl-alanine of fowl plague virus multiplication. Virology 11: 676-698.

45. Adams S, Xing Z, Li J, Mendoza K, Perez D, Reed K, Cardona C (2013) The effect of avian influenza virus NS1 allele on virus replication and innate gene expression in avian cells. Mol Immunol 56: 358-368.

46. Green IJ (1962) Serial propagation of influenza B (Lee) virus in a transmissible line of canine kidney cells. Science 138: 42-43.

47. DuBridge RB, Tang P, Hsia HC, Leong PM, Miller JH, Calos MP (1987) Analysis of mutation in human cells by using an Epstein-Barr virus shuttle system. Mol Cell Biol 7: 379-387.

48. Hoffmann E, Stech J, Guan Y, Webster RG, Perez DR (2001) Universal primer set for the full-length amplification of all influenza A viruses. Arch Virol 146: 2275-2289.

49. Neumann G, Watanabe T, Ito H, Watanabe S, Goto H, Gao P, Hughes M, Perez DR, Donis R, Hoffmann E, Hobom G, Kawaoka Y (1999) Generation of influenza A viruses entirely from cloned cDNAs. Proc Natl Acad Sci USA 96: 9345-9350.

50. Niwa H, Yamamura K, Miyazaki J (1991) Efficient selection for high-expression transfectants with a novel eukaryotic vector. Gene 108: 193-199.

51. Nao N, Kajihara M, Manzoor R, Maruyama J, Yoshida R, Muramatsu M, Miyamoto H, Igarashi M, Eguchi N, Sato M, Kondoh T, Okamatsu M, Sakoda Y, Kida H, Takada A (2015) A Single Amino Acid in the M1 Protein Responsible for the Different Pathogenic Potentials of H5N1 Highly Pathogenic Avian Influenza Virus Strains. PLoS One 10: e0137989.

52. Baudin F, Bach C, Cusack S, Ruigrok RW (1994) Structure of influenza virus RNP. I. Influenza virus nucleoprotein melts secondary structure in panhandle RNA and

exposes the bases to the solvent. EMBO J 13: 3158-3165.

53. Elster C, Larsen K, Gagnon J, Ruigrok RWH, Baudin F (1997) Influenza virus M1 protein binds to RNA through its nuclear localization signal. J Gen Virol 78: 1589-1596.

54. Watanabe K, Handa H, Mizumoto K, Nagata K (1996) Mechanism for inhibition of influenza virus RNA polymerase activity by matrix protein. J Virol 70: 241-247.

55. Ye Z, Liu T, Offringa DP, McInnis J, Levandowski RA (1999) Association of influenza virus matrix protein with ribonucleoproteins. J Virol 73: 7467-7473.

56. Ye ZP, Baylor NW, Wagner RR (1989) Transcription-inhibition and RNA-binding domains of influenza A virus matrix protein mapped with anti-idiotypic antibodies and synthetic peptides. J Virol 63: 3586-3594.

57. Wakefield L, Brownlee GG (1989) RNA-binding properties of influenza A virus matrix protein M1. Nucleic Acids Res 17: 8569-8580.

58. Bui M, Whittaker G, Helenius A (1996) Effect of M1 protein and low pH on nuclear transport of influenza virus ribonucleoproteins. J Virol 70: 8391-8401.

59. Huang X, Liu T, Muller J, Levandowski RA, Ye Z (2001) Effect of influenza virus matrix protein and viral RNA on ribonucleoprotein formation and nuclear export. Virology 287: 405-416.

60. Martin K, Helenius A (1991) Nuclear transport of influenza virus ribonucleoproteins: the viral matrix protein (M1) promotes export and inhibits import. Cell 67: 117-130.

61. Whittaker G, Bui M, Helenius A (1996) Nuclear trafficking of influenza virus ribonuleoproteins in heterokaryons. J Virol 70: 2743-2756.

62. Whittaker G, Kemler I, Helenius A (1995) Hyperphosphorylation of mutant influenza virus matrix protein, M1, causes its retention in the nucleus. J Virol 69: 439-445.

63. Shishkov AV, Goldanskii VI, Baratova LA, Fedorova NV, Ksenofontov AL, Zhirnov OP, Galkin AV (1999) The in situ spatial arrangement of the influenza A virus matrix protein M1 assessed by tritium bombardment. Proc Natl Acad Sci USA 96: 7827-7830.

64. Wang S, Zhao Z, Bi Y, Sun L, Liu X, Liu W (2013) Tyrosine 132 phosphorylation of influenza A virus M1 protein is crucial for virus replication by controlling the nuclear import of M1. J Virol 87: 6182-6191.

65. Ward AC (1997) Virulence of influenza A virus for mouse lung. Virus Genes 14: 187-194.

66. Campbell PJ, Kyriakis CS, Marshall N, Suppiah S, Seladi-Schulman J, Danzy S, Lowen AC, Steel J (2014) Residue 41 of the Eurasian avian-like swine influenza a virus matrix protein modulates virion filament length and efficiency of contact transmission. J Virol 88: 7569-7577.

67. Elleman CJ, Barclay WS (2004) The M1 matrix protein controls the filamentous phenotype of influenza A virus. Virology 321: 144-153.

68. Rott R, Orlich M, Scholtissek C (1982) Differences in the multiplication at elevated temperature of influenza virus recombinants pathogenic and nonpathogenic for chicken. Virology 120: 215-224.

69. O'Donnell CD, Vogel L, Matsuoka Y, Jin H, Subbarao K (2014) The matrix gene segment destabilizes the acid and thermal stability of the hemagglutinin of pandemic live attenuated influenza virus vaccines. J Virol 88: 12374-12384.

70. Morimoto K, Hooper DC, Spitsin S, Koprowski H, Dietzschold B (1999) Pathogenicity of different rabies virus variants inversely correlates with apoptosis and rabies virus glycoprotein expression in infected primary neuron cultures. J Virol

73: 510-518.

71. Halder UC, Bhowmick R, Roy Mukherjee T, Nayak MK, Chawla-Sarkar M (2013) Phosphorylation drives an apoptotic protein to activate antiapoptotic genes: paradigm of influenza A matrix 1 protein function. J Biol Chem 288: 14554-14568.

72. Munster VJ, Schrauwen EJ, de Wit E, van den Brand JM, Bestebroer TM, Herfst S, Rimmelzwaan GF, Osterhaus AD, Fouchier RA (2010) Insertion of a multibasic cleavage motif into the hemagglutinin of a low-pathogenic avian influenza H6N1 virus induces a highly pathogenic phenotype. J Virol 84: 7953-7960.

73. Soda K, Asakura S, Okamatsu M, Sakoda Y, Kida H (2011) H9N2 influenza virus acquires intravenous pathogenicity on the introduction of a pair of di-basic amino acid residues at the cleavage site of the hemagglutinin and consecutive passages in chickens. Virol J 8: 64.

74. Veits J, Weber S, Stech O, Breithaupt A, Graber M, Gohrbandt S, Bogs J, Hundt J, Teifke JP, Mettenleiter TC, Stech J (2012) Avian influenza virus hemagglutinins H2, H4, H8, and H14 support a highly pathogenic phenotype. Proc Natl Acad Sci USA 109: 2579-2584.

75. Guntaka RV, Richards OC, Shank PR, Kung HJ, Davidson N (1976) Covalently closed circular DNA of avian sarcoma virus: purification from nuclei of infected quail tumor cells and measurement by electron microscopy and gel electrophoresis. J Mol Biol 106: 337-357.

76. Hoffmann E, Neumann G, Hobom G, Webster RG, Kawaoka Y (2000) "Ambisense" approach for the generation of influenza A virus: vRNA and mRNA synthesis from one template. Virology 267: 310-317.

77. Zuker M (2003) Mfold web server for nucleic acid folding and hybridization

prediction. Nucleic Acids Res 31: 3406-3415.

78. Hausmann S, Garcin D, Delenda C, Kolakofsky D (1999) The versatility of paramyxovirus RNA polymerase stuttering. J Virol 73: 5568-5576.

79. Mehedi M, Falzarano D, Seebach J, Hu X, Carpenter MS, Schnittler HJ, Feldmann H (2011) A new Ebola virus nonstructural glycoprotein expressed through RNA editing. J Virol 85: 5406-5414.

80. Mehedi M, Hoenen T, Robertson S, Ricklefs S, Dolan MA, Taylor T, Falzarano D, Ebihara H, Porcella SF, Feldmann H (2013) Ebola virus RNA editing depends on the primary editing site sequence and an upstream secondary structure. PLoS Pathog 9: e1003677.

81. Ratinier M, Boulant S, Combet C, Targett-Adams P, McLauchlan J, Lavergne JP (2008) Transcriptional slippage prompts recoding in alternate reading frames in the hepatitis C virus (HCV) core sequence from strain HCV-1. J Gen Virol 89: 1569-1578.

82. Volchkov VE, Becker S, Volchkova VA, Ternovoj VA, Kotov AN, Netesov SV, Klenk HD (1995) GP mRNA of Ebola virus is edited by the Ebola virus polymerase and by T7 and vaccinia virus polymerases. Virology 214: 421-430.

83. Wagner LA, Weiss RB, Driscoll R, Dunn DS, Gesteland RF (1990) Transcriptional slippage occurs during elongation at runs of adenine or thymine in Escherichia coli. Nucleic Acids Res 18: 3529-3535.

84. Gott JM, Emeson RB (2000) Functions and mechanisms of RNA editing. Annu Rev Genet 34: 499-531.

85. Thomas SM, Lamb RA, Paterson RG (1988) Two mRNAs that differ by two nontemplated nucleotides encode the amino coterminal proteins P and V of the

paramyxovirus SV5. Cell 54: 891-902.

和文要旨

高病原性鳥インフルエンザ (HPAI) ウイルスは家禽に感染すると高い病原性を示し甚大な経済的被害をもたらすとともに、時にヒトに感染し重篤な肺炎を引き起こす。HPAI ウイルスの病原性発現には複数の因子が関与しており、HPAI ウイルスの中でも各宿主に対する病原性は株によって異なる。HPAI ウイルスの病原性決定因子についてはこれまでに多くの研究がなされているが、未だ不明な点が多い。

H5 または H7 亜型の表面糖タンパク質ヘマグルチニン (HA) を有する低病原性鳥インフルエンザウイルスが家禽の間で受け継がれると、時に HA の開裂部位に連続する塩基性アミノ酸を獲得し、ニワトリに対して高い病原性を示す HPAI ウイルスとなる。この HA 開裂部位の連続する塩基性アミノ酸は HPAI ウイルスの病原性決定因子としてよく知られているが、塩基性アミノ酸が挿入されるメカニズムならびに野鳥や家禽から分離される HPAI ウイルスが H5 または H7 亜型に限定されている理由は不明である。

第一章では、HPAI ウイルスの HA の開裂性以外の病原性決定因子の解明を目的として、2 株の HPAI ウイルス A/duck/Hokkaido/WZ83/2010 (H5N1) (WZ83) と A/duck/Hokkaido/WZ101/2010 (H5N1) (WZ101) を解析した。WZ83 と WZ101 は遺伝的に非常に近縁であり、RNA ポリメラーゼの一つである PB1 の 317 番目とマトリックスタンパク質 M1 の 43 番目のアミノ酸が異なっているのみであるが、ニワトリ、アイガモ、マウスに対する病原性に違いが見られた。WZ83 と WZ101 を静脈内または鼻腔内に接種したニワトリは、WZ83 を経鼻接種した 1 羽を除いて全羽死亡したが、WZ101 接種群は WZ83 接種群よりも短時間で死亡した。この病原性の違いはアイガモでより顕著であり、WZ101 を接種した個

体は死亡もしくは重篤な臨床症状を示したのに対し、WZ83 接種群は無症状もしくは軽度の臨床症状を示したのみであった。さらに、マウスに対しても WZ101 は WZ83 より高い病原性を示した。リバースジェネティクス法によって M または PB1 遺伝子を 2 株の間で入れ替えたウイルスを作出し、その病原性を解析したところ、WZ83 と WZ101 のニワトリとアイガモに対する病原性の違いは M1 の 43 番目のアミノ酸により決定されていることが判明した。一方、マウスに対する病原性の違いには PB1 の 317 番目のアミノ酸も関与していた。M1 の 43 番目のアミノ酸は動物に対する病原性に加えて、*in vitro* での増殖能及び感染細胞内における M1 の安定性にも関与していた。

第二章では、HA 開裂部位に塩基性アミノ酸が挿入されるメカニズムの解明を目的として、HA 開裂部位をコードするウイルスゲノム RNA 配列への塩基挿入を解析した。実験的にニワトリで継代することで HA 開裂部位に塩基性アミノ酸を獲得し、HPAI ウイルスになったことが報告されている低病原性鳥インフルエンザウイルス A/whistling swan/Shimane/499/83 (H5N3) (Shimane) の継代前および継代途中の HA 遺伝子配列を使用した。開始コドン、Shimane の HA 開裂部位周辺をコードする塩基配列 (28-30 塩基) および開始コドンを欠いたルシフェラーゼ遺伝子を連結し、その両端に A/Puerto Rico/8/1934 (H1N1) (PR8) HA 遺伝子の非翻訳領域をもつレポータープラスミドを構築した。このプラスミドと PR8 のポリメラーゼ及び核タンパク質 NP を発現するプラスミドを QT6 細胞に導入し、ウイルス RNA の転写・複製過程において HA 開裂部位周辺をコードする配列 (28 または 29 塩基) に塩基挿入が起きた時に発現するルシフェラーゼの活性を測定することにより、塩基挿入の頻度を定量的に検出した。その結果、HA 開裂部位周辺の RNA 配列に塩基挿入が生じること、ならびにアデニンの連続配列が塩基挿入の頻度を増加させることが示された。また、RNA の二次

構造予測から、Shimane の HA 開裂部位周辺をコードする RNA 配列はアデニンとグアニンによって形成されるループ構造を有していることが予測され、ループ構造の大きさと塩基挿入の頻度には関連があることが示唆された。さらに、ウイルス粒子中に含まれるウイルスゲノム RNA における塩基挿入の有無及び頻度を次世代シークエンサーを用いて解析した。その結果、Shimane の HA 開裂部位のアルギニンの 1 つ前 (スレオニン) または 2 つ前 (グルタミン酸) のアミノ酸をコードするコドン中に、高頻度にアデニンの挿入が見られた。また、Shimane の HA 開裂部位周辺をコードする領域に多く含まれるアデニンとグアニンの存在は、複数の塩基挿入が生じた際に塩基性アミノ酸 (アルギニンまたはリジン) をコードするコドン (AAA、AAG、AGA、AGG) を生じやすくさせると推測された。

本研究によって得られた知見は、カモに対する病原性が低下した HPAI ウイルスの拡散を監視するための鳥インフルエンザサーベイランスの重要性を示すとともに、家禽の間で広がっている低病原性鳥インフルエンザウイルスの高病原性化のリスクを予測する一助となるものと期待される。